UNIVERSITY „POLITEHNICA" OF BUCUREŞTI
FACULTY OF ELECTRICAL ENGINEERING
DEPARTMENT OF ELECTRICAL MACHINES, MATERIALS AND DRIVES

PHD THESIS
-SUMMARY-

ELECTROMAGNETIC PHENOMENA MODELING OF NANOSTRUCTURED DIELECTRIC MATERIALS

PhD Student: As. drd. ing. Elena - Laura ANDREI (căsăt. ENACHE)
PhD Supervisor: Prof. dr. ing. Florin CIUPRINA

Bucharest
2022

TABLE OF CONTENTS

KEY WORS: nanostructuring, interface, polymeric nanocomposites, nanoparticles, dielectric relaxation, electrical conduction, dielectric spectra, numerical modeling, electrostatic regime, quasi-stationary electric regime, inverse problem, optimization

CHAPTER I

INTRODUCTION

This following doctoral thesis presents the field of polymeric nanocomposite materials for electrical engineering, also known as nanodielectrics, focusing on the understanding of how nanostructuring, meaning the chemical structure changing of a material at the nanometer level, influences its behavior under the action of an electromagnetic field in different environmental conditions. Nanostructuring is not just the addition of nanometric fillers in a polymeric matrix, but all changes in structure that occur at the nanometer level in a material (at distances between 1 and 100 nm). The research conducted in the PhD studies analyzed nanostructured dielectric materials based on polymers whose structure was modified by the addition of nanoparticles. It was also analyzed how the exposure of these materials to various environmental factors (temperature and humidity) further influences the change in their structure and, implicitly, their electrical and dielectric performance. For the individual characterization of nanometric components of nanostructured materials, called nanostructures, things get even more complicated because changing the structure at the nanometric level creates a new entity (component), the interface area. In this area the geometric characteristics as well as the chemical and physical properties are different from the initial state of each component of the total system. This area is very important because, being at the level of nanometers, it gets to have a huge share in the nanostructured material. Deciphering the properties and structure of this interface area has so far proved to be the way to improve the properties of the core polymer, as nanoscale interactions between individual components are manifested in the macroscopic performance of the final system. As there is no experimental determination to illustrate how each molecule, with each atom, respectively with each electron, in this interface area interacts with the electromagnetic field, modeling is the main approach to highlight these interactions that manifest at the nanometer level.

The main objective of the doctoral thesis was to analyze and model the dielectric spectra of polymeric nanocomposite materials and make physical and numerical models that highlight the dynamics of electrical charges in these dielectric materials following the phenomena of conduction and electrical polarization. To achieve the proposed objective, measurements were made by dielectric spectroscopy considering different environmental factors such as temperature and humidity. The dielectric spectra obtained provided, on the one hand, information necessary to understand the behavior of nanostructured dielectric materials under the influence of an electromagnetic field, and on the other hand, they were a source of information necessary for numerical modeling. Another important objective of the thesis was to highlight the importance of dielectric spectroscopy in the electrical characterization of nanostructured dielectric materials, by highlighting the electrical charges inside and their dynamics.

The first chapter presents the importance of the chosen topic and the purpose of the research, the main objectives of this paper, as well as a brief presentation of the chapters in this thesis.

The second chapter presents a bibliographic study of the current state of research for nanostructured materials. Since the central theme of this paper is modeling the phenomena that occur in nanostructured dielectric materials due to the application of an electric field, the last part of the documentary study on the current state of nanostructured dielectric materials is dedicated to models developed for these materials.

Chapter III begins with a presentation of theoretical considerations concerning dielectric spectroscopy, the method used to analyze the interaction between the electromagnetic field and materials. Then the chapter III presents the experimental

determinations made on several sets of samples of nanostructured dielectric materials, based on polyvinyl chloride, polyethylene or polypropylene with different nanofillers (silicon dioxide, titanium dioxide, aluminum trioxide or microfibrils). cellulose), to follow the effects of nanostructuring on the phenomena of electrical polarization and electrical conduction based on the dielectric spectra of these materials.

Chapter IV focuses on the characterization and structural modeling of a polymeric nanocomposite material among those analyzed in the previous chapter, namely a nanostructured material based on polypropylene (PP) and silicon dioxide (SiO_2). Starting from the chemical structure of this material and based on some of the structural models in the literature, the fourth chapter proposes a structural model that highlights the chemical and physical bonds that could be formed in the interface area between nanoparticles and polymer. With this structural model, the types and concentrations of dipoles in the different regions of the nanodielectric are estimated, which then determine the values of the electrical permittivities in each region of the material. These values are then used to develop an electrostatic numerical model of the PP-SiO_2 nanodielectric.

Chapter V analyzed the influence of frequency on the dynamics of electric charge by developing a numerical model in quasi-stationary electric regime which highlighted the dispersive nature of the interface, modeled the interface to highlight its role in changing frequency-dependent dielectric properties in a nanostructured material based on polypropylene and silicon dioxide. This model, based on the information found in the literature and the results of the research presented in the previous chapters, allows the estimation of the electrical properties of the interface area, at room temperature or as a result of temperature variations. At the end of the chapter, we analyze the use of the proposed model on several types of polymeric nanocomposite materials with fillers of different shape and composition (titanium dioxide in the form of anatase and rutile) or different basic polymer matrix (polyethylene), in order to develop and validate this model.

At the end of the paper, **Chapter VI**, the conclusions of this doctoral thesis are highlighted, the original contributions to the research are gathered and the possible ways forward for the future are presented to further develop this topic, modeling electromagnetic phenomena in nanostructured dielectric materials.

CHAPTER II

STATE OF ART IN RESEARCH OF NANOSTRUCTURED MATERIALS

Nanostructured materials are solid structures made of at least one structural element (grains / clusters, crystallites or molecules) of the order of nanometers (1 to 100 nm) [1]. These structural elements are called nanostructures [1].

In recent years, nanostructured materials have generated widespread interest in research and industry due to their physic -chemical characteristics (melting point, moisture resistance, mechanical strength, thermal and electrical conductivity, electrical permittivity, electrical stiffness, etc.) superior to individual components in which are obtained. This major advantage of nanostructured materials comes from the "custom made" character of "ordinary" materials obtained by modifying their structure at the level of atom or molecule.

Depending on the type of nanostructure contained, most nanostructured materials can be classified into four broad categories [2, 3]:

1. Nanostructured materials containing carbon-based nanostructures

These are nanostructured materials that contain nanostructures made of carbon atoms and that are spherical (fullerenes, nanodiamonds), foil (graphene) or tubular (carbon nanotubes) [2].

2. Nanostructured materials containing inorganic nanostructures

In the field of inorganic nanostructures, spherical nanoparticles are of particular importance because their obtaining in the laboratory as well as their mass production is easier and cheaper than other nanostructures, such as carbon nanotubes [4].

3. Nanostructured materials containing organic nanostructures

Dendrimers, liposomes, micelles, polymeric nanoparticles, etc. are commonly known as organic nanostructures. These nanostructures are mainly made of organic materials, excluding carbon-based nanostructures [2].

4. Other composite nanostructured materials

This category includes the other types of nanostructures present in nanostructured materials that have not been previously presented [2], namely: nanocrystalline materials [5], nanoporous materials [6], nanofibrous materials (nanofibrils) [7, 8], nanowires, nanoflowers, nanowires [9-11].

Another type of classification of nanostructured materials according to the materials used for the matrix is the following: nanocomposites with ceramic matrix (Al_2O_3 and SiO_2 being the most used), nanocomposites with metal matrix (metal alloys based on Cu, Al, Au, Ag, Mg and others) and polymeric matrix nanocomposites (thermoplastic / thermosetting polymers such as polyethylene, polypropylene, polyester, PVC, epoxy resin, polyamide, etc.) [12].

Given the classification presented above, depending on the type of nanostructure contained and the type of matrix used, the materials to be analyzed in this doctoral thesis are nanostructured materials based on thermoplastic polymers with inorganic (nanoparticles) and organic (microfiber) components.

2.1.   NANOSTRUCTURED MATERIALS FOR ELECTRICAL ENGINEERING

In recent years, the electric field has seen an amazing expansion. With the development of this field, due to the need for more and more efficient materials in terms of electrical properties, the field of nanostructured materials used in electrical engineering has developed (nanostructured materials with conductive properties, semiconductor nanostructured materials, nanostructured materials with magnetic properties, materials with electrical insulating properties), making nanotechnology have a major impact on industry and research [13].

Nanostructuring of **materials with electrical insulating properties** used in electrical engineering can be done in two ways: by adding nanometer-sized fillers (nanoparticles) into pure electrical insulating materials (polymers), in which case these materials are called polymeric nanocomposite materials, or by exposing electrical insulating materials to various external environmental factors (temperature, humidity, pressure), radiation or electrical stress (intense electric field).

2.2.1. **Nanostructuring – adding particles in polymeric materials**

Polymeric nanocomposites are composite materials whose basic polymeric matrix is a thermoplastic polymer (PE, PP, PA, PS, PVC, PDMS) or thermoset (epoxy resin) in which

particles of nanometric size (1-100 nm) are dispersed. These nanometer-sized particles are called nanofillers or nanoparticles.
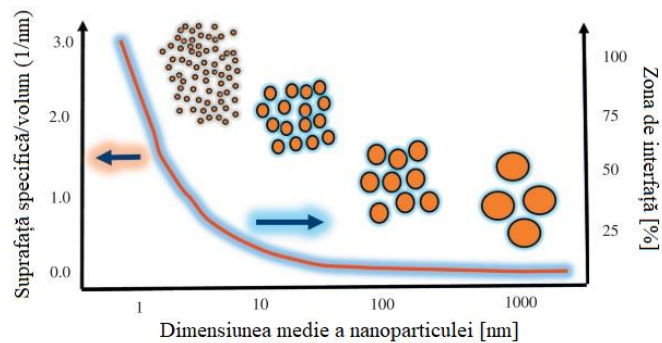
Fig. 2.1. The relationship between the specific surface area and the volume of the composite compared to the average size of the nanoparticles [14].

Understanding and controlling the properties of these new materials, polymeric nanocomposites, can lead to their use in various applications in the electrical field. But for this it is necessary to know not only the properties of the base polymer and the nanofillers, but also the properties of the area that is formed between these two constituents of the new material, an interface area. The interface area, although it has a thickness, and therefore a volume, well defined, is mentioned in the literature only by the word "interface", which will be used throughout this thesis. As can be seen in ***Fig. 2.1.***, The area of the specific surface is very large if the size of the filling decreases, so the interface area will be implicitly larger.

Among the applications already existing on the world market and with a huge potential are those in the electrical and electronics industry (sensors, information storage, cable insulation), but also those in energy storage (supercapacitors, battery electrodes, membranes for combustion cells).

2.2.2. Nanostructuring – defects existing in polymeric materials

The existence or appearance of various defects in polymeric materials also causes changes in the structure at the atomic level. Resistance to electrical stresses (normal stresses when equipment is in operation or surges caused by electrical phenomena, network equipment, etc.) can be seen over time in the case of live electrical insulating polymeric materials either in the form of partial discharges or by the appearance of trees. water or electric.

2.2. MODELS FOR NANOSTRUCTURED MATERIALS FOR ELECTRICAL ENGINEERING

The properties of the interface area cannot be determined experimentally, but only modeled, primarily by graphical representations (to be able to "see" it, to determine quantitatively how much it extends in each volume) or by representations of the structure to provide information on its physic-chemical behavior. A variety of models have been developed for this interface area, including the following:

1. Model of the diffuse electric double layer in the interface [15].

2. Dual layer interface model [16].

3. Multi-core interface model [17].

4. Interphase volume model [18].

5. Power law for interfaces model [19]

6. The structural model developed within ELMAT [20, 21].

7. The ENIC model [20, 22].

8. 2D interface model [23].

CHAPTER 3

CHARACTERIZATION AND MODELING OF NANOSTRUCTURED POLYMERIC MATERIALS USING DIELECTRIC SPECTROSCOPY ANALYSIS

In this chapter, the method of dielectric spectroscopy is firstly described, by presenting the measurement principle, the phenomena in materials highlighted by dielectric spectroscopy and the models used for the analysis and processing of experimental data. The rest of the chapter presents a series of experimental studies, performed based on determinations by dielectric spectroscopy, which highlights the influence of nanostructuring on the dynamics of electrical charges in the tested materials.

3.1.   DIELECTRIC SPECTROSCOPY – MEASUREMENT PRINCIPLE

Dielectric spectroscopy (DS), or impedance spectroscopy, is a method of measuring the dielectric properties of a material as a function of the frequency of the electric field. The measurement principle used in dielectric spectroscopy is presented below. In a measuring cell, a planar sample having thickness d is placed between two electrodes, having area A, forming a planar capacitor. A sinusoidal voltage U_0 of frequency f equal to $\omega/2\pi$ is applied to the formed capacitor, where ω is the pulsation [24]. This voltage causes a current of current I_0 of the same frequency, but which is out of phase with the voltage at an angle φ.

The relationships between voltage, current intensity and phase shift between them are determined by the electrical properties of the sample (relative permittivity and electrical conductivity), but also by the shape of the sample (electrode area and distance between electrodes or sample thickness).

3.2.   DIELECTRIC SPECTROSCOPY - PHENOMENAS

For the interpretation of the experimental results obtained by dielectric spectroscopy, as well as for the elaboration of the numerical models of the studied nanodielectrics, a very important aspect is the understanding of the phenomena of conduction and electrical polarization.

The measurements by dielectric spectroscopy within the research carried out for the elaboration of this doctoral thesis were performed on nanostructured materials based on polymers, in the frequency range 10^{-2} - 10^6 Hz. The typical shape of the dielectric spectrum of the materials tested in this frequency range is that shown in Figure 3.1.

This typical variation of the real part and the imaginary part of the complex permittivity signal the presence of a dielectric relaxation for medium or high frequencies and a conduction for low frequencies. Part of the low frequency spectrum may contain, in addition to the component due to conduction, a component due to polarization at the electrode.
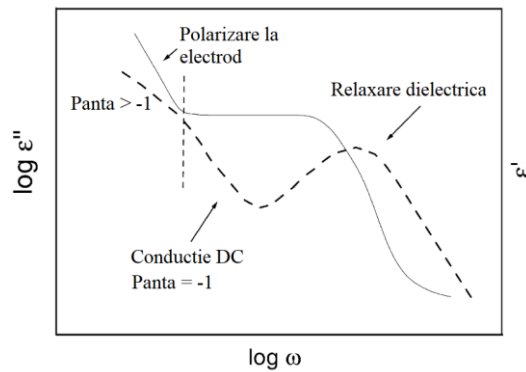
Fig. 3.1. Typical variation for ε' (solid line) and ε'' (dashed line) with frequency in polymeric dielectrics [25].

Dielectric relaxation represents the cessation of polarization processes existing in the material over certain frequencies of the electric field, called proper relaxation frequencies. Dielectric relaxation is the process of restoring equilibrium within a system following the removal of an action of the electric field [26], meaning the cessation of a certain polarization mechanism at a certain proper relaxation frequency. For the frequency range considered in this doctoral thesis, the polarization of inhomogeneity ceases over the industrial frequencies, and the orientation polarization ceases over the radio frequencies.

3.3.   MODELS FOR ANALYSIS AND PROCESSING OF EXPERIMENTAL DATA

Dielectric relaxation processes are usually analyzed using approximation functions. Starting from the classic Debye function, different formulas have been suggested for both frequency and time domain to describe the experimentally observed dielectric spectra, where the symmetry of the relaxation peak disappears. The most important of these approaches were discussed in this doctoral thesis.

The analysis of nanostructured dielectric materials from an electrical point of view involves in addition to the analysis with the help of functions of approximation of the experimental data of the whole system and an individual analysis of the components (polymer matrix, filling, interface area). The latter analysis is usually needed in the modeling of nanostructured materials that aims to predict certain behaviors under the action of an electromagnetic field. In this sense, various empirical models for the analysis and processing of experimental data have emerged, gathered under the name of *effective medium theories* (EMT).

3.4.   INORGANIC NANOPARTICLES INFLUENCE ON THE DIELECTRIC RESPONSE OF VINYL POLYCHLORIDE NANOCOMPOSITES

In the process of obtaining the samples from ICECHIM Bucharest, the polymeric PVC matrix was mixed in a Brabender LabStation plastograph using the direct mixing method, with inorganic fillers (SiO_2, TiO_2, Al_2O_3).

For the experimental determination of the real and imaginary part of the relative electrical permittivity (ε_r' and ε_r''), of the loss factor (tg δ) and of the real part of the electrical conductivity (σ') we used a NOVOCONTROL dielectric spectrometer, equipped with ZGS measuring cell. The measurements were performed in the frequency range 10^{-2} - 10^6 Hz for three temperature values, once for an increasing temperature variation and once for a decreasing temperature variation.

Table 3.1. Polymeric nanocomposites based on polyvinyl chloride with inorganic nanoparticles [27].

NO	SAMPLE	MASS CONCENTRATIONS FROM MIXTURES
1	**pure PVC**	100% **PVC**
2	**PVC-SiO₂ 5%**	95% **PVC**, 5% **SiO₂**
3	**PVC-TiO₂ 5%**	95% **PVC**, 5% **TiO₂**
4	**PVC-Al₂O₃ 5%**	95% **PVC**, 5% **Al₂O₃**

In order to use the dielectric spectra to analyze the dynamics of electrical charges in nanostructured dielectric materials, the experimental results were further processed using the WinFIT software application from Novocontrol. This software application allows the approximation of the dielectric spectra with the Havriliak – Negami (HN) function which contain also a term for DC conductivity, the equation considered for the approximation of the variation with the frequency of the complex permittivity being [28]:

$$\underline{\varepsilon}_r(\omega) = \varepsilon'_r(\omega) - j\varepsilon''_r(\omega) = -j\left(\frac{\sigma_{DC}}{\varepsilon_0\omega}\right)^N + \sum_k \left[\frac{\Delta\varepsilon_k}{(1+(j\omega\tau_{HN})^\alpha)^\beta} + \varepsilon_\infty\right] \qquad (3.1)$$

3.4.1. Dielectric response analysis of PVC nanocomposites

First, an increase of ε_r' values can be observed in all three PVC-based nanocomposites compared to pure PVC, especially at low frequencies. This increase in electrical permittivity (ε_r') may be due to new dipoles introduced into the basic polymeric matrix (PVC) by nanostructuring [29]. The highest values for ε_r' were obtained for PVC-Al₂O₃ nanocomposites, while PVC-TiO₂ nanocomposites show values close to the base polymer. Regarding tg δ, in figure 3.2. (b) lower losses can be observed for PVC-TiO₂ nanocomposites compared to pure PVC and the other two nanocomposites, for the whole frequency range [30].
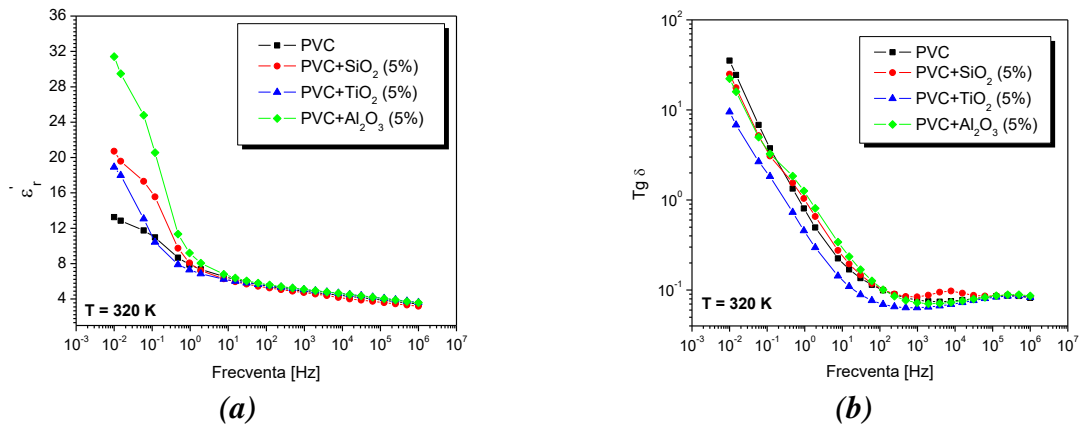
Fig. 3.2. Frequency variation of the real part of the complex permittivity *(a)* and tangent of the loss angle *(b)* for pure PVC and PVC-based nanocomposite at 320 K [30].

3.4.2. Influence of temperature variations on the dielectric properties of PVC nanocomposites

Representative dielectric spectra do not show a typical frequency dependence of the real and imaginary part of the complex permittivity. This behavior has also been found in other nanostructured dielectric materials and indicates a so-called "low frequency dispersion". [30, 25]. Also, the results presented show how the characteristic frequency of LFD increases as the temperature increases from about 10^{-1} Hz to 310 K, to 10^1 Hz to 340 K.
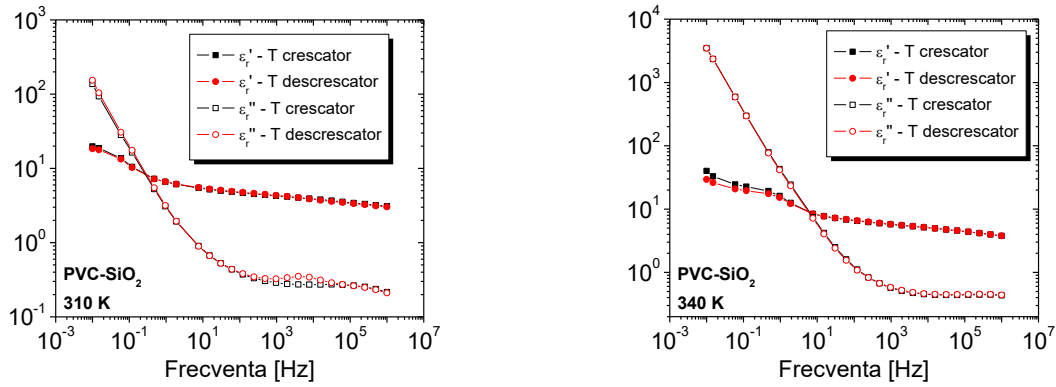
Fig. 3.3. Variation of the real and imaginary part of the complex permittivity with the frequency for the PVC-SiO$_2$ nanocomposite, determined for a decreasing and increasing temperature, at 310 K and 340 K [30].

Another remark regarding the dielectric spectra in the above figures is the small difference between the dielectric response obtained for an increasing temperature compared to that obtained for a decreasing temperature. Different dielectric spectra at the increasing temperature with respect to the decreasing temperature would emphasize the influence of the material "history" on the dielectric behavior. This difference due to the "history" of the materials tested depends on the measurement temperature and the type of filler added to PVC [30].

It can be noticed that the increase of temperature leads to an increase of real relative permittivity and loss tangent at all frequencies and for both neat PVC and all tested PVC nanocomposites [30].
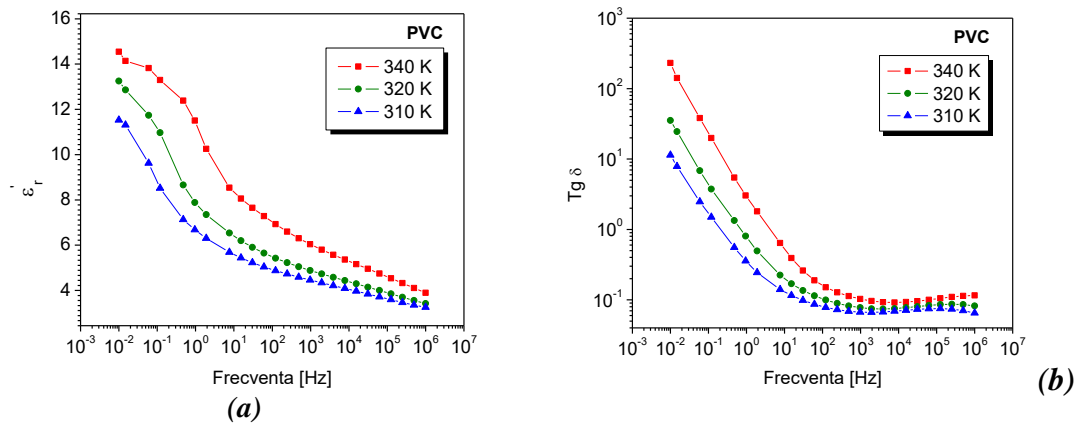
Fig. 3.4. Frequency variation of ε$_r$' *(a)* and of tg δ *(b)*, for neat PVC at different temperatures for a decreasing temperature [30].
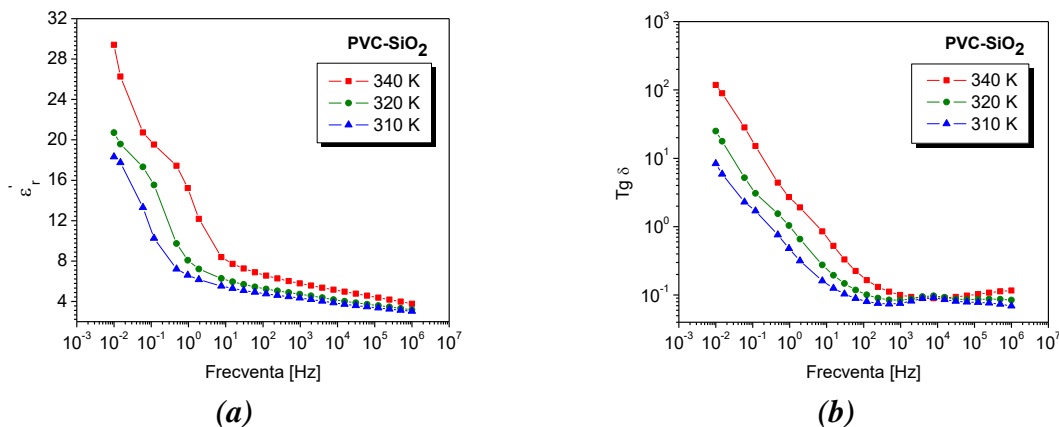
Fig. 3.5. Frequency variation of ε$_r$' (a) and of tg δ (b), for PVC-SiO$_2$ nanocomposite at different temperatures for a decreasing temperature [30].

3.4.3. Influence of temperature variations on the electric conductivity of PVC-TiO$_2$ nanocomposites

The presence of TiO$_2$ nanoparticles in PVC leads to an increase in the electrical insulating performance of the polymer, the decrease in nanocomposite conductivity compared to the pure polymer being more than an order of magnitude at temperatures higher than 320 K. The values of exponent N of the first term 0.79 and 0.91, which, according to the model proposed in [129, 133-135], indicates a predominantly electronic conduction by hopping in both pure PVC and nanocomposite. The activation energies resulting from the approximation of these variations are 0.92 eV for PVC and 1.03 eV for nanocomposite. These values indicate a difficulty in conducting by hopping to the nanocomposite relative to the undoped polymer [31, 32].

From the approximation of the variations σ' with the frequency using the universal law proposed by *Jonscher* (**Table 3.3.**) results values for σ_{DC} very close to those previously obtained with equation HN (3.1) (**Table 3.2.**) from the analysis of the ε_r'' variations with the frequency for the studied materials. The activation energy of electronic conduction by hopping resulting from the use of the universal law proposed by *Jonscher* has similar values to that obtained with the Havriliak-Negami equation which contains a factor for the DC conductivity. Using either of the two approaches to extract DC conductivity values leads to the same results.

Table 3.2. DC conductivity values according to the approximation of the variation ε_r'' (ω) for the three analyzed temperatures [31]

	σ_{DC} [S/m]		
	310 K	320 K	340 K
PVC	$9{,}52 \cdot 10^{-11}$	$3{,}78 \cdot 10^{-10}$	$2{,}08 \cdot 10^{-9}$
PVC-TiO$_2$ (5%)	$3{,}05 \cdot 10^{-11}$	$9{,}65 \cdot 10^{-11}$	$9{,}06 \cdot 10^{-10}$

Table 3.3. DC conductivity values according to the approximation of the variation $\sigma'(\omega)$ for the three analyzed temperatures [32].

	σ_{DC} [S/m]		
	310 K	320 K	340 K
PVC	$5{,}54 \cdot 10^{-11}$	$2{,}2 \cdot 10^{-10}$	$1{,}36 \cdot 10^{-9}$
PVC-TiO$_2$ (5%)	$1{,}54 \cdot 10^{-11}$	$4{,}8 \cdot 10^{-11}$	$6{,}26 \cdot 10^{-10}$

3.5. NANOSTRUCTURING INFLUENCE ON DIELECTRIC RESPONSE OF POLYETYLENE NANOCOMPOSITES

The samples tested in this study were made at ICECHIM Bucharest from polymeric nanocomposites based on polyethylene (PE) with inorganic titanium dioxide fillings in the form of anatase (TiO$_2$A) or rutile (TiO$_2$R) and aluminum trioxide (Al$_2$O$_3$) [27].

Table 3.4. Polyethylene-based polymeric nanocomposites with inorganic fillers.

NO	SAMPLE	MASS CONCENTRATIONS FROM MIXTURES
1	**pure PE**	95% **PE**, 5% **PE-g-AM** (1% AM)
2	**PE-TiO$_2$R 2%**	93% **PE**, 5% **PE-g-AM** (3% AM), 2% **TiO$_2$R**
3	**PE-TiO$_2$R 5%**	90% **PE**, 5% **PE-g-AM** (3% AM), 5% **TiO$_2$R**
4	**PE-TiO$_2$A 2%**	93% **PE**, 5% **PE-g-AM** (3% AM), 2% **TiO$_2$A**
5	**PE-TiO$_2$A 5%**	90% **PE**, 5% **PE-g-AM** (3% AM), 5% **TiO$_2$A**
6	**PE-Al$_2$O$_3$ 2%**	93% **PE**, 5% **PE-g-AM** (3% AM), 2% **Al$_2$O$_3$**

The obtaining method is the direct mixing method.

The NOVOCONTROL dielectric spectrometer, equipped with the ZGS measuring cell in the same frequency range and at different temperatures, was used for the experimental determination of the real and imaginary part of the relative electrical permittivity (ε_r' and ε_r'').

3.5.1. Influence of titanium dioxide nanoparticles on dielectric response of PE nanocomposites

The shape of the inorganic filler influence, sphere or cylinder, on ε_r' is distinguished by the fact that nanofillers of spherical shape led to a higher relative permittivity than the cylindrical ones, regardless of the concentration in which they are added. The variation of ε_r'' with the frequency of the electric field is different depending on the type of nanofiller added in polyethylene, the relaxation and conduction processes occurring differently.

3.5.2. Temperature influence on dielectric properties of PE nanostructured materials with different concentrations of titanium dioxide

As the temperature increases, the values of the real part of the relative permittivity become lower for the whole frequency range for both pure polyethylene and nanocomposite. This decrease in ε_r' values with temperature is due to thermal agitation and thermal dilatation and has been observed in our previous studies on polyethylene-based nanocomposites [25, 20, 33].

The frequency variation of the imaginary part of the ε_r'' complex permittivity shows a considerably weaker relaxation activity for pure polyethylene compared to nanocomposites.

The variation of ε_r'' with temperature and frequency for the nanocomposite with spherical fillers is more complex, indicating the following dielectric relaxation events: a segmental relaxation that occurs at low frequencies (Fj), an interfacial relaxation that occurs at medium frequencies (Fm) and another relaxation at the level of chemical bonding due to the lateral groups present at high frequencies (Fî). All these relaxation processes are temperature dependent, being controlled and thermally activated.

The thermal activation energies for the Fj and Fm relaxations present in the nanodielectrics were obtained 0.81 eV and 1.25 eV for the 2% TiO_2A nanocomposite and 1.01 eV and 1.04 eV for the 5% TiO_2A nanocomposite, respectively. Similarly, the thermal activation energy was obtained for the main peak observed for PE in the frequency range $10 - 10^{-3}$ Hz whose value was 1.03 eV.

(a)   *(b)*
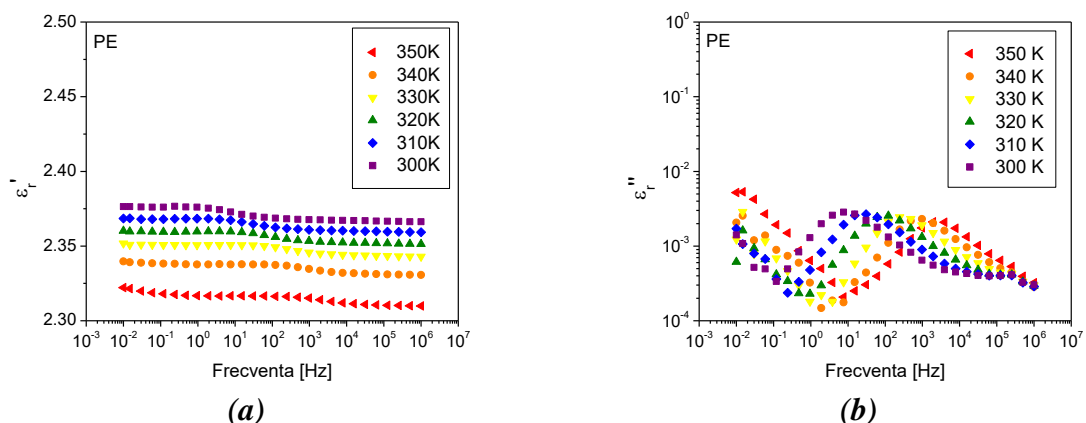
Fig. 3.6. Variation of the real *(a)* and imaginary *(b)* part of the complex permittivity with frequency for the polymer matrix, PE for a decreasing temperature variation.
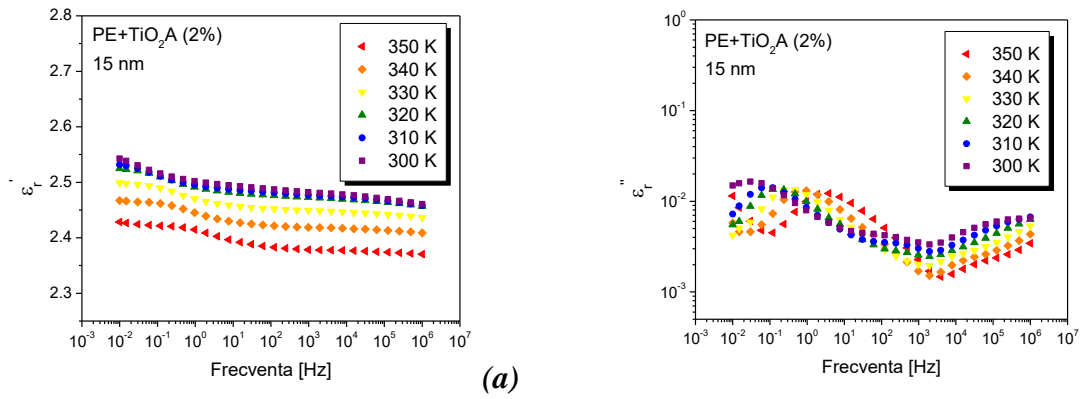
Fig. 3.7. Variation of the real *(a)* and imaginary *(b)* part of the complex permittivity with frequency for the polymer matrix, PE-TiO$_2$A 2% for a decreasing temperature variation.

3.5.1. Water and Heat Exposure Influence on Dielectric Response of PE-Al$_2$O$_3$ Nanocomposites

The values of the real part of the permittivity, ε_r' for the nanocomposites analyzed as the temperature increases in the entire frequency range, and for all the conditions tested (initially, wet and for the three stages of heat exposure). The main responsible for this behavior is thermal agitation, which prevents the orientation of the dipoles in the different regions present in the nanostructured material. In the variation with frequency of ε_r'', the appearance of three dielectric relaxation mechanisms can be observed for all three experimental conditions tested. To illustrate these three processes of electrical polarization, the dielectric spectra were approximated with the Havriliak-Nagami (HN) equation.
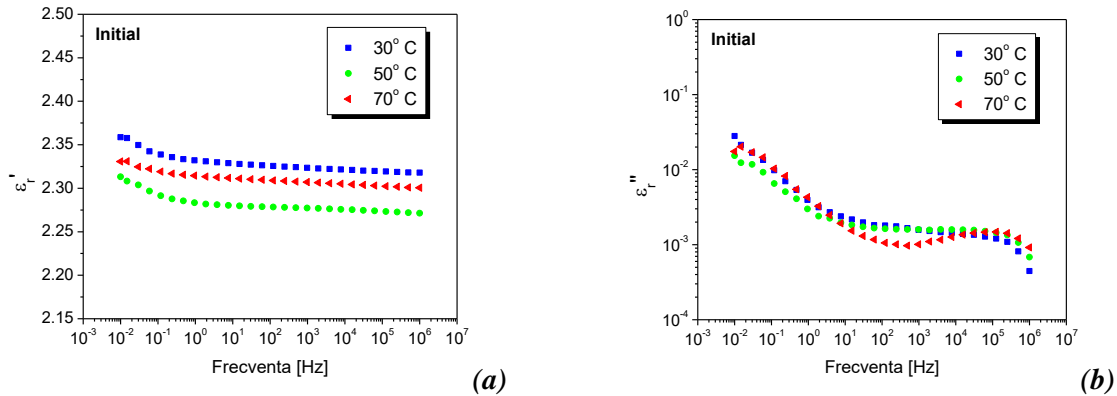
Fig. 3.8. Variation of the real *(a)* and imaginary *(b)* part of the complex permittivity with the frequency for the PE-Al$_2$O$_3$ nanocomposite in the initial state, at different temperatures [33].
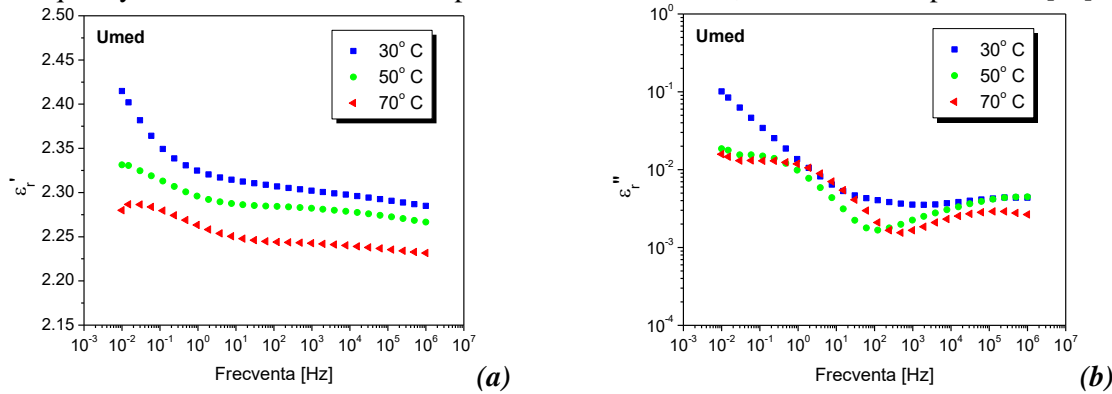
Fig. 3.9. Variation of the real *(a)* and imaginary *(b)* part of the complex permittivity with the frequency for the PE-Al$_2$O$_3$ nanocomposite affected by humidity, at different temperatures [33].
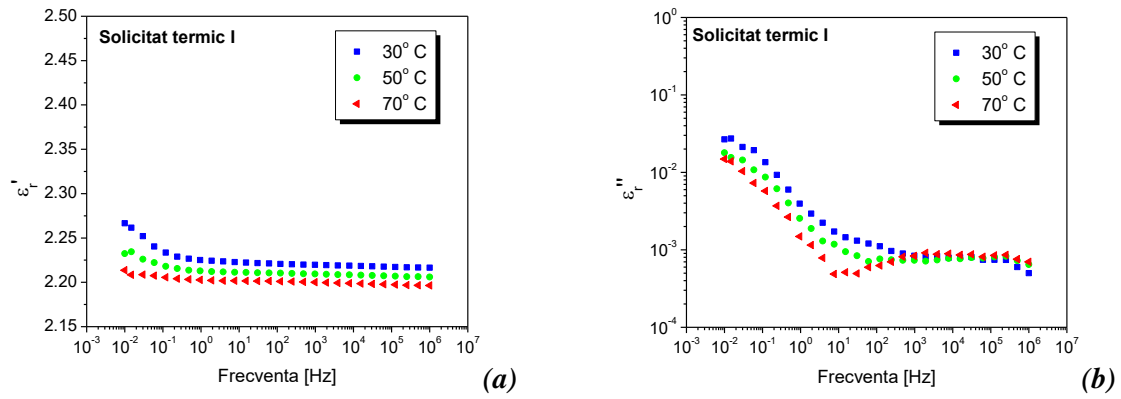
Fig. 3.10. Variation of the real *(a)* and imaginary *(b)* part of the complex permittivity with the frequency for the PE-Al$_2$O$_3$ nanocomposite affected by the first thermal exposure, at different temperatures [33].

The influence of humidity and heat exposure on the electrical properties of the PE-Al$_2$O$_3$ nanocomposite shows small differences in ε_r' values between the "wet" and "initial" states and between the three heat exposure stages and the 'initial' state. The small differences in ε_r' values, around 1% after exposure to water and less than 5% after exposure to heat, together with the small differences in the behavior of dielectric losses after the samples have been moistened and thermally aged, high dielectric stability of PE-Al$_2$O$_3$ (2%) nanocomposite.

3.6. NANOSTRUCTURING INFLUENCE ON DIELECTRIC PROPERTIES OF POLYPROPYLENE NANOCOMPOSITES

The third set of samples that were tested is polymeric nanocomposites based on polypropylene (PP) with inorganic fillers of silicon dioxide (SiO$_2$), titanium dioxide (TiO$_2$) and aluminum trioxide (Al$_2$O$_3$) in a concentration of 5% made in within ICECHIM Bucharest. [27].

Table 3.5. Polypropylene-based polymeric nanocomposites with inorganic nanofillers

NO	SAMPLE	MASS CONCENTRATIONS FROM MIXTURES
1	**pure PP**	95% **PP,** 5% **PP-g-AM** (1% AM)
2	**PP-SiO$_2$ 5%**	90% **PP,** 5% **PP-g-AM** (1% AM), 5% **SiO$_2$**
3	**PP-TiO$_2$ 5%**	90% **PP,** 5% **PP-g-AM** (1% AM), 5% **TiO$_2$**
4	**PP-Al$_2$O$_3$ 5%**	90% **PP,** 5% **PP-g-AM** (1% AM), 5% **Al$_2$O$_3$**

To compare the dielectric response of some nanocomposites based on PP with inorganic fillers with the dielectric response of some nanocomposites also based on PP, but with organic fillers, a fourth type of samples was made, nanostructured polymeric materials containing microfibrils. organic cellulose. The method of production is the direct mixing method for both types of PP-based nanocomposites.

Table 3.6. Polypropylene-based polymeric nanocomposites with organic nanofillers

| NO	SAMPLE	MASS CONCENTRATIONS FROM MIXTURES
1	**pure PP**	95% **PP,** 5% **PP-g-AM** (1% AM)
2	**PP-fiber A 5%**	90% **PP,** 5% **PP-g-AM** (1% AM), 5% **fiber A**
3	**PP-fiber B 5%**	90% **PP,** 5% **PP-g-AM** (1% AM), 5% **fiber B**
4	**PP-fiber C 5%**	90% **PP,** 5% **PP-g-AM** (1% AM), 5% **fiber C**

The dielectric spectra of the complex permittivity were determined in the frequency range

15

between 10^{-2} and 10^6 Hz in the temperature range 300 K - 350 K using a NOVOCONTROL dielectric spectrometer, equipped with the ZGS measuring cell.

In the case of this study, in addition to the determinations by dielectric spectroscopy, the use of complementary measurement techniques (thermogravimetric analysis, chemiluminescence and analysis of mechanical properties) better outlines the point of view on a certain electrical behavior found in nanostructured dielectric materials analyzed in this doctoral thesis. it also gives validity to the study.

3.6.1. Influence of different types of nanoparticles on dielectric response of PP nanocomposites

From the addition of nanoparticles to the basic polymeric matrix, polypropylene, it is observed that the ε_r' values of the nanocomposites with nanoparticles of SiO_2, TiO_2 and Al_2O_3 are higher compared to those of the basic matrix (***Fig. 3.11. (a)***). This is due to the high frequencies of the dipoles forming due to the nanostructuring of the material and to the low frequencies due to the MWS polarization produced in the interface area between the nanofiller and the polymer, whose area increases with the filler concentration according to the multilayer model proposed by *Tanaka* [17].

(a)   *(b)*
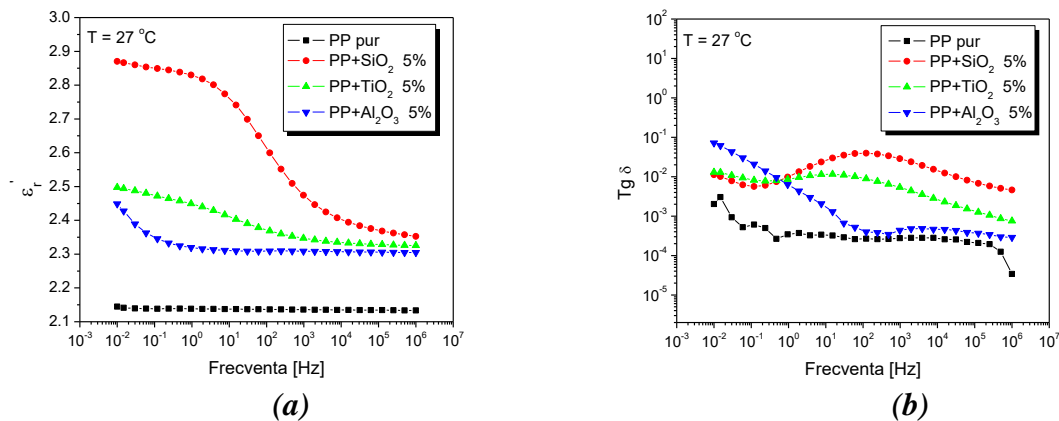
Fig. 3.11. Variation of the real part of the complex permittivity *(a)* and of the loss tangent *(b)* with the frequency for PP-based nanocomposites with different types of inorganic nanofillers (SiO_2, TiO_2 and Al_2O_3) at 27 ˚C [8].

As for the loss factor, as can be seen in Figure 3.11 (b) it increases by up to two orders of magnitude by adding nanoparticles to the base polymer over the entire frequency range. The smallest increase, in an order of magnitude, is in the case of nanocomposites with Al_2O_3 particles in the frequency range 10^2 - 10^6 Hz.

For the PP-SiO_2 nanocomposite, the dielectric relaxation process becomes important and is signaled by the existence of a peak in the frequency variation of the values of the imaginary part of the electrical permittivity correlated with the decrease of the values of the real part of the electrical permittivity. In the literature this type of relaxation is known as α relaxation.

Figure 3.12 shows a comparison between the variation of the dielectric spectra of the PP-SiO_2 nanocomposite for the increase and decrease of the temperature. The figure below clearly shows how the direction of temperature variation strongly influences the dielectric behavior of the nanocomposite.

This displacement of the maximum values of the imaginary part of the permittivity can be attributed to two phenomena that occur simultaneously and influence each other: thermal activation of the dipole orientation due to increased molecular mobility with temperature and change in water content in nanocomposite due to increase / decrease of applied temperature. The weight of the two phenomena in the displacement of dielectric relaxation is another question mark, which leads in the near future to perform more tests by dielectric spectroscopy and not only, which highlights on the one hand a purely activated behavior thermal (drying

the material and then measuring by dielectric spectroscopy with increasing and decreasing temperature variations), and on the other hand a pure dielectric behavior influenced by humidity (gradual wetting of the material, repetition of dielectric spectroscopy tests at 300 K, repetition of TGA analysis). After performing these tests, the energy of pure thermal activation or dielectric relaxation with humidity can be calculated.

(a)   *(b)*
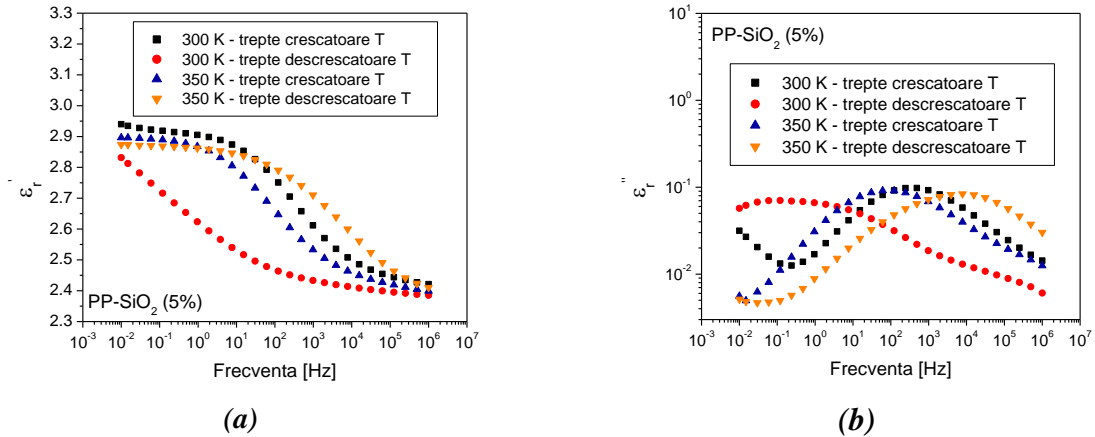
Fig. 3.12. Variations of ε_r' *(a)* and ε_r'' *(b)* with frequency for the PP-SiO₂ nanocomposite at 300 K and 350 K for increasing and decreasing temperature variation [34].

3.6.2. Influence of organic nanoparticles on dielectric properties of PP nanostructured materials

The results obtained for nanostructured PP-based materials with organic fillers highlight the improvement of the mechanical properties of the composites PP - cellulose microfibers compared to the matrix polymer, especially the modulus of elasticity. It has also been observed that the dielectric properties (both the real part of the complex permittivity and the tangent of the loss angle), although they increase slightly by the introduction of microfibrils in PP, remain at values that are characteristic of good dielectrics, in a wide range frequency. At the same time, a stability of the dielectric properties could be noticed with the increase of the temperature.

(a)   *(b)*
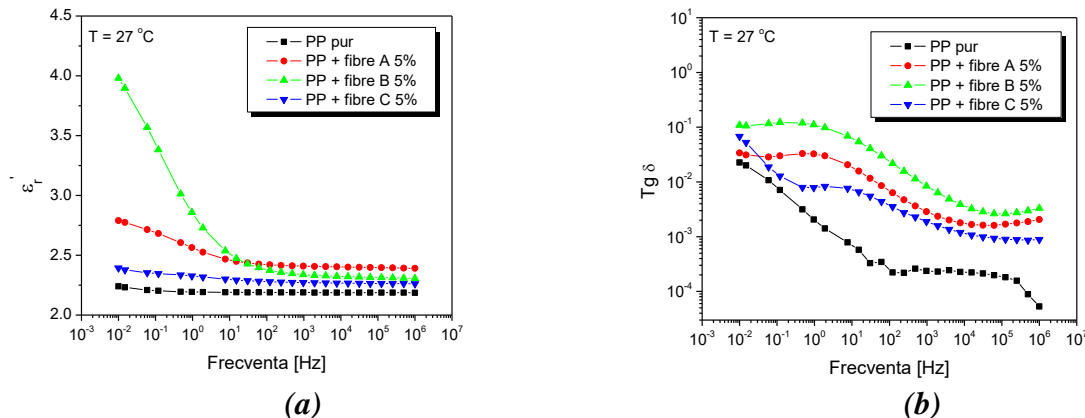
Fig. 3.13. Variation of the real part of the complex permittivity *(a)* and the tangent of the loss angle *(b)* with the frequency for PP-based composites with different types of organic fillers (fibers A, B and C) at 27 ˚C [8].

CHAPTER 4

MULTIPHYSICS MODELING OF PP-SiO$_2$ NANOCOMPOSITES

In this chapter, the presentation of the modeling of nanostructured materials is continued, being analyzed only one of the materials presented in Chapter III, namely the PP-SiO$_2$ nanocomposite. The main purpose of this chapter is to highlight the interface of this nanostructured material in terms of free electrical charges, dipoles, chemical and physical bonds that may exist at this interface and are responsible for that behavior observed through spectrum analysis. dielectric.

4.1. MULTIPHYSICS MODELING - THEORETICAL BACKGROUND

Further the stages of multiphysics modeling are presented, starting from the conceptual model to the numerical modeling itself facilitated using modern and current software.

Conceptual modeling is the first step of modeling, and it establishes the geometric model and the physical model. Therefore, in the conceptual modeling, the structure of the modeled object (materials, shapes, dimensions, component parts and their assembly) are described and the principle of operation is analyzed. After the conceptual modeling, through which the geometric and physical model of the analyzed object was made, follows the ***mathematical modeling*** where the problem is formulated from a mathematical point of view. Usually, this problem involves solving a system of partial differential equations. Once the problem has been formulated correctly, it will be solved. At the beginning, it is preferable to have an analytical solution of the problem which it should be much simplified compared to the original one. In most cases, ***analytical solutions*** are obtained based on much simplified geometric models, such as the 1D or 2D geometric model. Obtaining accurate solutions, in the case of complicated configurations, involves using computers to evaluate the solution, thus following a ***numerical approach***. In this paper, the finite element method was used for numerical analysis. Currently, this method is the most widely used compared to other numerical methods for field analysis. After the elaboration of the model, the evaluation and verification follow. ***Verification*** assumes that the model has been constructed in accordance with the requirements given by the mathematical formulation of the problem, and ***validation*** assumes that the previous formulation is correct, in accordance with reality [35].

4.2. STRUCTURAL MODEL OF PP-SIO$_2$ NANOCOMPOSITE

4.2.1. Chemical and physical bonds dipoles in the PP-SiO$_2$ nanocomposite

PP-SiO$_2$ nanocomposite is a composite material consisting of polypropylene - PP and inorganic silicon dioxide nanoparticles - SiO$_2$ 5% concentration which have a diameter of $d = 15$ nm.

To represent the interface area at the surface of the silica nanoparticle for the case of the nanocomposite PP-SiO$_2$ we started from *Todd's* model [19]. Thus, three distinct regions were considered in the nanocomposite, namely: ***region 1*** represented by identical spheres with diameter $d = 2r$ (inorganic SiO$_2$ nanoparticles), ***region 2*** represented by the nanoparticle interface - polymer matrix with thickness $g_i = g_1 + g_2 + g_3$, consisting of 3 layers with different dimensions, ***region 3*** represented by the polymeric matrix (***Fig. 4.1.***).
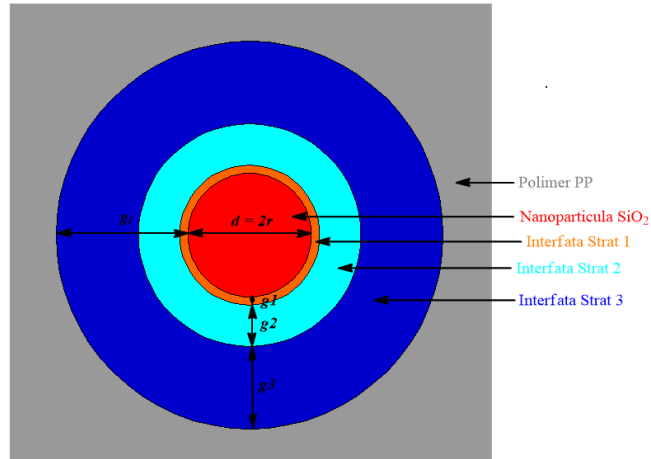
Fig. 4.1. The three distinct areas of the structure of the PP-SiO$_2$ nanocomposite.

Therefore, the interface area was considered having the following three layers [21, 34] (***Fig. 4.1***):

1. **Layer 1**

The first layer is considered to have molecular dimensions (~ 1 nm) and consists of adsorbed ions or dipoles (physically - by Van der Waals forces or chemically - by adsorption and the creation of chemical bonds). Thus, the bonds that can be formed in layer 1 are:

- Chemical bonds that form between the SiO$_2$ nanoparticle and the PP chains via AM (hydrogen bonds between the O-H hydroxyl groups adsorbed on the surface of the nanoparticles (strongly hydrophilic) during the technological process of obtaining and AM molecules, as well as covalent bonds double and single $C = O, H - H, O - O$ and $C - O$) (***Fig. 4.2.***).
- Most chemical bonds between the SiO$_2$ nanoparticle and water ($H - O - H$), adsorbed during the manufacturing process or in the environment (***Fig. 4.2.***).
- **C-C, C-H** type chemical bonds that come from the ends of PP chains, but which in the first layer are in negligible quantity (***Fig. 4.2.***) [21].
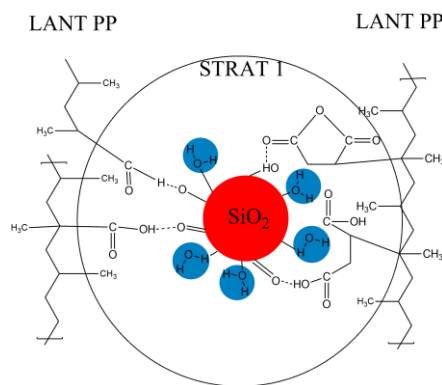
Fig. 4.2. The chemical and physical bonds that can be formed in layer 1.

2. **Layer 2**

From the second layer the polymer changes its conformation and / or mobility of the polymer chain due to the presence of the nanofiller. In this regard, the second layer is assigned:

- ends of polymeric PP chains, by chemical bonds of type $C - H$, $C - C$ (coming from the functional groups of PP: CH, CH2, CH3) (*Fig. 4.3.*);
- chemical bonds established between PP grafted with AM and nanoparticle of type $O - H$, $C - O$ and $C = O$ (*Fig. 4.3.*). Hydrogen bonds are formed between the H atoms at the ends of the PP chains in layer 2 and the hydroxyl groups adsorbed on the surface of the nanoparticles. In layer 2 a branch of the polymer chains is formed between which electrostatic forces are established, which have a tendency to order the PP chains.
- the rest of the chemical bonds coming from the water adsorbed by the nanocomposite,
- $H - O - H$ -type bonds (Fig. 4.3.).
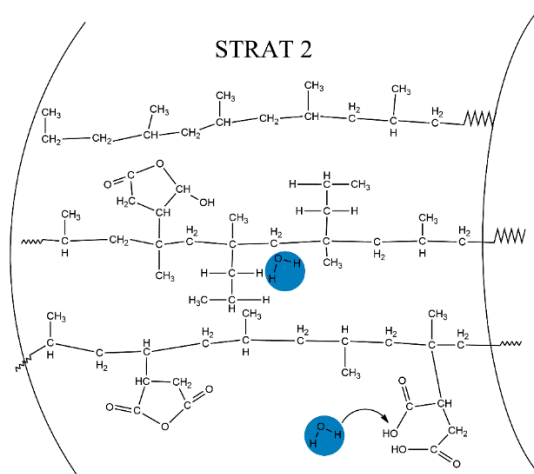
Fig. 4.3. The chemical and physical bonds that can be formed in layer 2.

3. **Layer 3**

The third layer is a region that binds and interacts superficially with the second layer. This layer is assigned:

- macromolecular PP clusters that become more and more disordered from the first layer to the third and between which chemical bonds are established, especially covalent bonds of type **C-C, C-H**. After finishing the interface area, PP regains its semicrystalline structure (*Fig. 4.4.*);
- residues of PP grafted with AM, so chemical bonds of type $O - H$, $C - O$ and $C = O$ (*Fig. 4.4.*).
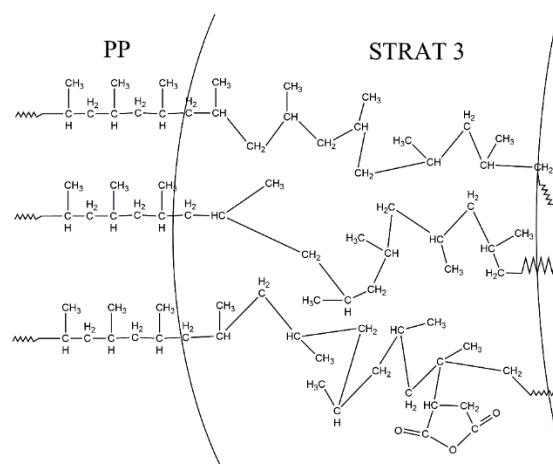
Fig. 4.4. The chemical and physical bonds that can be formed in layer 3.

4.2.2. Dielectric properties model of PP-SiO$_2$ nanocomposite interface area

The structural model of the PP-SiO$_2$ nanocomposite considers the possible types of electric dipoles that could occur as previously presented, as well as the structure of this material in the interface area. The following ones are the assumptions of the model for calculating the number of electric dipoles for each layer of the nanoparticle-polymer interface to be used to extract the electrical permittivity of the interface regions:

1. The **interface** is considered to have three layers of different thicknesses [17, 15, 21]:

$$g_{layer1} = 1 \text{ nm}, \ g_{layer2} = 5 \text{ nm}, \ g_{layer3} = 10 \text{ nm} \ ;$$

2. According to *Tanaka's* model [17], we will assume **the density of the interface area** equal to that of the matrix even after the introduction of nanoparticles:

$$\rho_{layer1} = \rho_{layer2} = \rho_{layer3} = \rho_{PP} = 0,9 \text{ g/cm}^3 \ ;$$

   The volumes of the interface layers are calculated based on the thicknesses considered for each, and then the masses corresponding to each layer of the interface are extracted.

3. We consider the **Debye model** [36] which assumes that there are no interactions between dipoles. The existence of free charges, electrons or ions does not affect their orientation according to the direction of the field with a certain frequency, and this simplifies the complexity of the model to achieve a first iteration of this structural model. At the same time, considering a Debye model can only be a starting point, because in reality the analyzed material is not completely homogeneous and may contain polar molecules that affect the short-distance motion of these related tasks.

4. In **layer 1** the existence of type electric dipoles shall be considered: **C$^{\delta+}$←O$^{\delta-}$, O$^{\delta-}$→H$^{\delta+}$, H$^{\delta+}$←O$^{\delta-}$→H$^{\delta+}$**.

5. In **layer 2** the existence of type electric dipoles shall be considered: **C$^{\delta-}$→H$^{\delta+}$, C$^{\delta+}$←O$^{\delta-}$, O$^{\delta-}$→H$^{\delta+}$, H$^{\delta+}$←O$^{\delta-}$→H$^{\delta+}$.**

6. In **layer 3** the existence of type electric dipoles shall be considered**: C$^{\delta-}$→H$^{\delta+}$, C$^{\delta+}$←O$^{\delta-}$, O$^{\delta-}$→H$^{\delta+}$**.

7. The following relationship will be used to calculate the relative permittivity of each interface layer (4.1).

$$\varepsilon_{r\_layer\_k} = 1 + \chi_{i\_layer\_k} + \chi_{o\_layer\_k}, \qquad k = 1, 2, 3 \tag{4.1}$$

   The ionic and orientation susceptibilities of each polar bond that form in each interface layer were calculated using the micro-macro relationship between local electrical polarizability, α and global electrical susceptibility, χ. The volume concentration of dipoles and ions participating in ionic polarization will be considered equal. ($N_i = N_o$).

8. The structural constant γ will be considered considering the symmetry or asymmetry of the molecules participating in the polarization phenomenon.

4.3. ELECTROSTATIC MODELING OF PP-SIO$_2$ NANOCOMPOSITE

This section presents an electrostatic numerical model of the PP-SiO$_2$ nanocomposite. This numerical model, called ENIC (from *electrostatic numerical with interface charge*), was developed to simulate the dielectric behavior of this nanocomposite material [20]. The numerical model is based on the structural model presented in the previous section. Thus, using the assumptions and dipoles related to the functional groups considered in the

nanoparticle-polymer interface, the relative permittivity values of each layer of the interface were first estimated. These values, together with those for the permittivities for PP and SiO₂, were used for the subdomains of the ENIC model. After constructing and solving the model, the numerical solution obtained was used to determine the equivalent permittivity of the PP-SiO₂ nanocomposite, and the value thus obtained was compared with that determined experimentally by dielectric spectroscopy.

The calculation of the equivalent permittivity was made starting from the determination of the total capacity of the nanocomposite which is constituted by an interconnection of elementary capacitors connected in series and in parallel [20, 22]. The electrical properties that must be imposed for the subdomains of the numerical model of the PP-SiO₂ nanocomposite, developed in electrostatic regime, are the electrical permittivity and the density of volumetric electric charge.

Subdomain	Electrical permittivity
PP	$\varepsilon_m = 2,2$
Interface - Layer 1	$\varepsilon_{I1} = 4,07$
Interface - Layer 2	$\varepsilon_{I2} = 2,56$
Interface - Layer 3	$\varepsilon_{I3} = 2,53$
Overlap layer 3	$\varepsilon_{I3} = 2,53$
SiO₂ Nanoparticle	$\varepsilon_p = 4$
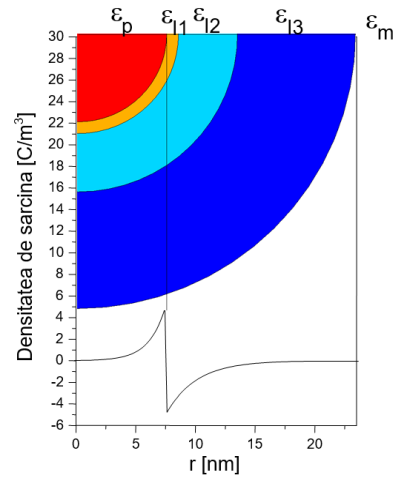
Fig. 4.5. Electric charge distribution and relative electrical permittivity for each subdomain considered in the numerical model.

The values of the electrical permittivity for each nanocomposite area (polymer matrix, three-layer interface area, interface layer overlap area and nanoparticle) were determined from the structural model described above and from the catalog data for PP and SiO₂. Knowing the volume concentration of the dipoles on each layer, the electrical permittivity of each area (subdomain) considered in the interface was estimated. The variation of the charge density from the polymer matrix to the nanoparticle through the interface area (***Fig. 4.5.***) was considered according to the models proposed by *Lewis* [15] and *Tanaka* [17]. Regarding the boundary conditions, Dirichlet conditions were imposed on the upper and lower face of the elementary cube (opposite planes xOy). On the symmetry planes, xOz and yOz, the Neumann condition was considered zero.

Numerical and experimental results were discussed considering that the numerical simulation was done in electrostatic regime while the determinations by dielectric spectroscopy were performed under the action of a harmonic electric field.

The variation of the electric field along a line perpendicular to the two armatures and passing through the centers of the nanoparticles is represented in ***Fig. 4.7*** for the PP-SiO₂ nanocomposite. This variation is represented by the two considered cases of the numerical problem: a numerical model in which no electric charge is considered and a model in which an exponential distribution of electric charge in the three layers of the interface area was considered. From ***Fig. 4.7*** can be seen the non-uniformity of the electric field variation in the PP-SiO₂ nanocomposite, but also its disturbance associated with the electric charge distribution in the interface area. Also, from the variation of the electric field its values are

higher in the interface area, in the layers near the nanoparticle, while in the nanoparticle it is very low.

(a)

(b)
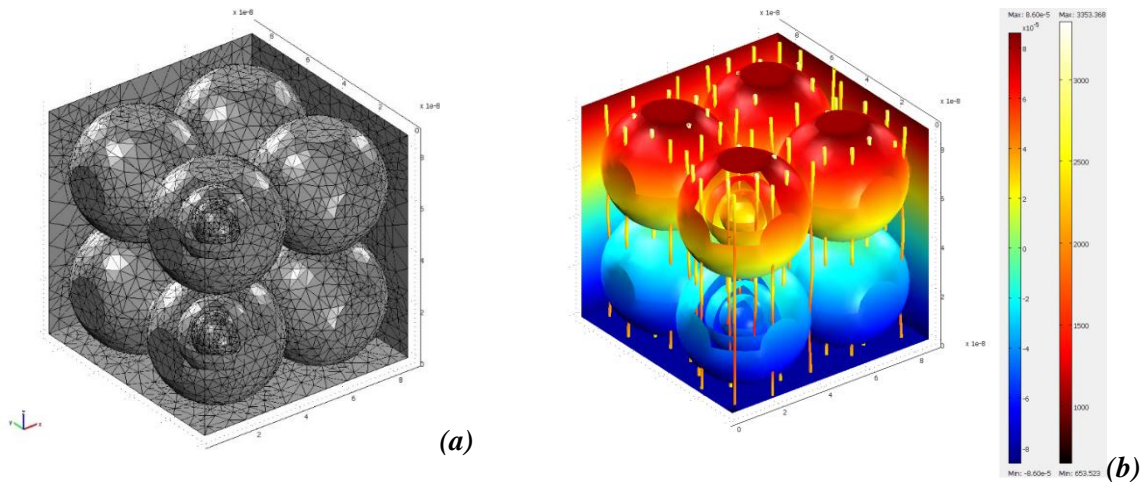
Fig. 4.6. Finite element discretization network of the 3D electrostatic field *(a)* and the distribution of the scalar electric potential (rainbow) and the electric field (tubes) *(b)* for the PP-SiO$_2$ nanocomposite.
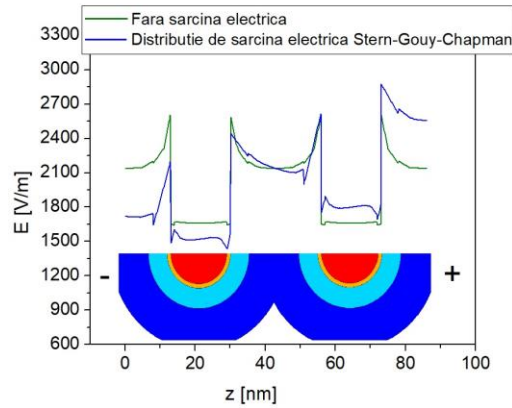
Fig. 4.7. Distribution of electric field strength along a line perpendicular to armature passing through nanoparticles for the PP-SiO$_2$ nanocomposite.

Table 4.1. Comparisons between equivalent relative permittivity values obtained using the ENIC and experimental model.

Effective permitivity	Numerical Model	Dielectric Spectroscopy	Relative error [%]
ENIC, no electric charge	2.46	**2.42 ($f = 10^6$ Hz)**	1.57
ENIC, with electric charge	2.86	**2.94 ($f = 10^{-2}$ Hz)**	2.63

The numerical solution obtained after postprocessing this model was used to estimate the equivalent permittivity of the PP-SiO$_2$ nanocomposite. As can be seen in **Table 4.1.** the relative errors for the effective electrical permittivity values are below 3%, which validates the assumptions made in both the structural and numerical models. By comparing the experimental values measured by dielectric spectroscopy with the estimates of the ENIC model, an interesting correlation can be seen from **Table 4.1**: at low frequencies (10^{-2} Hz), the measured values are approximated with an error of 2.63% of the values calculated with the ENIC model in the presence of the exponential electric charge distribution, while at high

frequencies (10^6 Hz) the measured values are comparable with an error of 1.57% with the values calculated with the ENIC model in the absence of electric charge.

CHAPTER 5

DIELECTRIC PROPERTIES ESTIMATION OF NANODIELECTRIC INTERFACE BY NUMERICAL MODELING AND DIELECTRIC SPECTROSCOPY

This chapter presents a method for estimating the frequency-dependent dielectric properties of the interface area that exist in polypropylene-based nanodielectrics with SiO_2 nanoparticles. This method is based on a quasi-stationary electrical model in 3D, where the subdomains of the nanocomposite (polymer matrix, nanoparticles and interface) are considered to be dispersive materials [37]. The main purpose of this method, which is basically an inverse problem, was to find the frequency-dependent dielectric properties of the interface, so that the modeling results, meaning the values of the real part of the effective electrical permittivity and the values of the dielectric loss factor, are close to the experimental results obtained by SD.

5.1.   DIELECTRIC PROPERTIES ESTIMATION OF NANODIELECTRIC INTERFACE OF PP-SIO$_2$ NANOCOMPOSITES AT ROOM TEMPERATURE

For numerical modeling of the PP-SiO_2 nanodielectric, spherical SiO_2 nanoparticles with 15 nm diameter were considered to be uniformly distributed in a PP polymer matrix, each nanoparticle being surrounded by a 10 nm thick interface region. The computational range of the simplified 3D model, similar to that of the Chapter IV model, is reduced to an elementary cell consisting of a cube containing eight nanoparticles.

The numerical model was made using COMSOL Multiphysics software, in quasi-stationary electric regime, assuming a linear, isotropic environment without permanent polarization and printed electric field. The solution to the problem was obtained by solving the fundamental equation of the quasi-stationary electric regime. To define the boundary conditions, the geometric symmetries of the xOz and yOz side planes are considered on the one hand, and thus the Neumann condition is imposed, and the Dirichlet condition is imposed on the upper and lower faces.

The material properties assigned to the three subdomains of the numerical model come either from experimental data or from the literature. It was assumed that in each subdomain there is a frequency-dependent electrical permittivity, while the electrical conductivity was considered constant in a first approximation. Thus, the electrical conductivity of PP was set $\sigma_{PP} = 10^{-17}$ S/m, as it resulted from our measurements with a Keithley 6517 electrometer (measurement of absorption / resorption currents). The electrical conductivities attributed to the nanoparticle and interface subdomains were between 10^{-15} S/m [38] and 10^{-13} S/m, respectively, based on experimental results from the literature. The electrical conductivity established for the subdomains assigned to the interface was considered higher than the required value of PP and nanoparticles, as some studies have shown in the case of polymeric materials with silica fillings an increase in quasi-DC conductivity for low frequencies, explaining this phenomenon by the existence of a double-electric layer in the interface [15] layer whose influence was also considered in the numerical model developed in electrostatic regime in Chapter IV.

The values of electrical permittivity were assigned to the subdomains of the model, by processing the results obtained by SD for PP and nanocomposite. Therefore, the main purpose of this study was to find the optimal values of the electrical permittivity to be assigned to the

nanoparticles and the interface area so that the results, meaning the variations with the frequency of the complex permittivity and the dielectric loss factor, the effective values for this nanodielectric, be as close as possible to the experimental results obtained by SD. To solve this problem, which is an inverse problem, in a first iteration we considered the nanodielectric as a bicomposite material, one component (A) being the polymeric matrix PP and the other component (B) nanoparticles surrounded by an interface area. Using either the asymmetric Bruggeman method or the Linear method, separately for the real part of the permittivity and for the imaginary part of the permittivity, we found, in the range 10^{-2} - 10^{6} Hz, the ε_B values for the B constituent (nanoparticles + interface), using the values for ε_{eff} and ε_A from SD measurements for PP-SiO$_2$ nanodielectric and pure PP, respectively.

In a first approximation (CASE I - ***Fig. 5.1. (a)***), the values of ε_B were assigned to both nanoparticles and interface subdomains.


Fig. 5.1. Assigning the values of the electrical permittivity found for component B to the subdomains of the geometric model: CASE I (a) and CASE II (b).

The numerical results obtained with this model made in COMSOL Multyphisics were compared with the experimental results obtained by SD and then the inverse problem was solved by adjusting the frequency dependent values for the permittivity assigned to the interface area and nanoparticles in order to minimize the error, calculated as Euclidean relative distance between numerical and experimental results (with relations 5.1 and 5.2).

$$err' = \frac{\left|\varepsilon'_{reff}(f) - \varepsilon'_{reff}(f)\right|}{\left|\varepsilon'_{reff}(f)\right|} \cdot 100 = \min \tag{5.4}$$

$$err'' = \frac{\left|\varepsilon''_{reff}(f) - \varepsilon''_{reff}(f)\right|}{\left|\varepsilon''_{reff}(f)\right|} \cdot 100 = \min \tag{5.5}$$

Figure 5.2 shows the frequency variations of ε'_r and tg δ obtained experimentally (squares) by dielectric spectroscopy and numerically (circles) by using the procedure described above, using the asymmetric Bruggeman (BA) model to approximate the values of electrical permittivity assigned to both the nanoparticle and the interface (CASE I). There is a similarity between the numerical and the experimental results in the case of the real part of the complex permittivity, with a relative error of less than 3%. Instead, in terms of the values for the loss factor, the shape of the variation of tg δ with frequency is similar for numerical and experimental results, but the numerical values are significantly lower than the experimental ones, except for the low frequencies close to 10^{-2} Hz where they are closer, the Euclidean error being ≈75%. To reduce this error, a scaling factor of the values obtained using the BA model will be used for the imaginary part of the permittivity and the values of the real part of the complex permittivity will be kept unchanged. The variation of the Euclidean relative distance indicates an optimal value of 3.9 of the scaling factor, for which the error is minimal, ε'_{reff} having a very small variation in this interval. Figure 5.2 shows a good correlation of the numerical results with those obtained by dielectric spectroscopy, the error being 23% for tg δ and 2,6% for ε'_r.
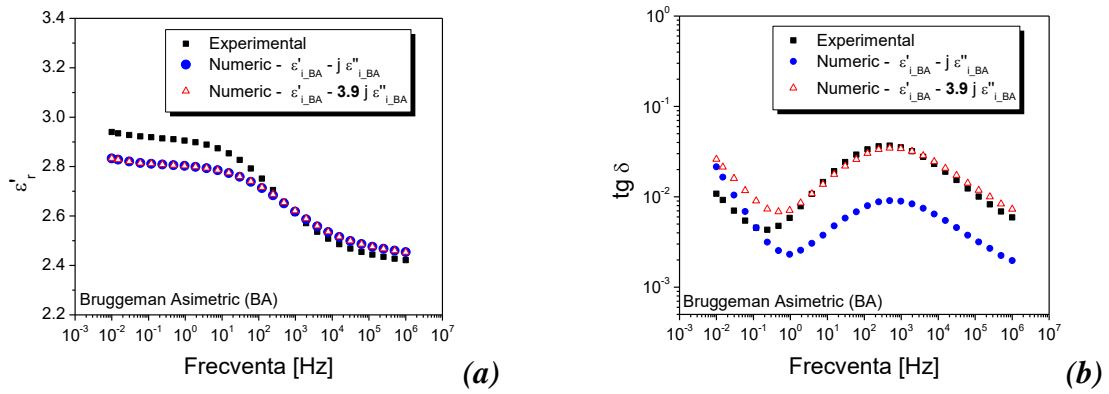
Fig. 5.2. Variation of ε'_r *(a)* and tg δ *(b)* with the frequency for the PP-SiO$_2$ nanocomposite obtained experimentally and numerically using the BA model [37] - CASE I.
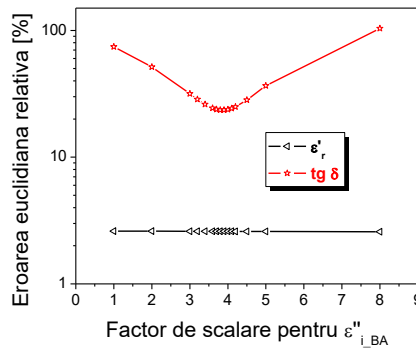
Fig. 5.3. Errors of numerical results as a function of the scaling factor used for the imaginary part of the permittivity obtained by formula BA [37] - CASE I.

In addition to the BA model, the linear model (LM) was also tested. The numerical results obtained with LM before any adjustment are close to the experimental results for both the real part of the complex permittivity, with an error of 1.9%, and for the loss factor, the error being 15%. [37].

However, so far, this dielectric behavior has been achieved by considering the nanoparticles and the interface as a whole, without emphasizing the contribution of each of them. Under these conditions, it was considered for a second iteration (**Fig. 5.1 (b)** - CASE II) of the numerical model that the values found for the real and the imaginary part be assigned only to the interface area, and for the subdomain of SiO$_2$ nanoparticles values are assigned constants taken from the literature in order to analyze which of the two subdomains has a more important role.

There were small differences between the results obtained for the two approaches (0.4% for ε'_r and 7.16% for tg δ), indicating that the dielectric behavior obtained using the adjusted BA model or the LM model can be attributed mainly to the interface area.

5.2. FREQUENCY DEPENDENT DIELECTRIC RESPONSE OF PP-SIO$_2$ NANOCOMPOSITE INTERFACE ZONE AT DIFFERENT TEMPERATURES

The study presented in this section aims to analyze the frequency-dependent dielectric response of the PP-SiO$_2$ nanocomposite interface region at different temperatures. The estimation of the dielectric properties of the interface was performed using the procedure described in the previous section.

The complex electrical permittivity of the interface resulted from the application of the optimization procedure using the LM model and two scaling factors, one for each of the components of the complex electrical permittivity.

Euclidean error values between numerical and experimental results for $\varepsilon'_{\text{reff}}(f)$ and $\varepsilon''_{\text{reff}}(f)$, obtained before and after the optimization of the complex permittivity of the interface, at each temperature analyzed, are presented in **Tables 5.1** and **5.2**.

Table 5.1. Euclidean error for the real part of the effective complex permittivity.

Euclidiean error $\varepsilon'_{\text{reff}}(f)$ [%]						
	300 K	**310 K**	**320 K**	**330 K**	**340 K**	**350 K**
Optimized	2,73	2,72	2,56	2,23	2,27	1,72
No optimized	12,25	12,24	12,75	13,21	13,43	14,33

Table 5.2. Euclidean error for the imaginary part of the effective complex permittivity.

Euclidiean error $\varepsilon''_{\text{reff}}(f)$ [%]						
	300 K	**310 K**	**320 K**	**330 K**	**340 K**	**350 K**
Optimized	14,89	15,35	16,22	15,37	15,80	14,31
No optimized	157,66	164,04	156,39	149,49	169,73	162,08

Once the two components of the frequency-dependent electrical permittivities for the interface area were estimated, they were compared with those obtained experimentally for the whole nanodielectric in order to emphasize the role of the interface on the dielectric behavior of the PP-SiO$_2$ nanocomposite.

(a) *(b)*
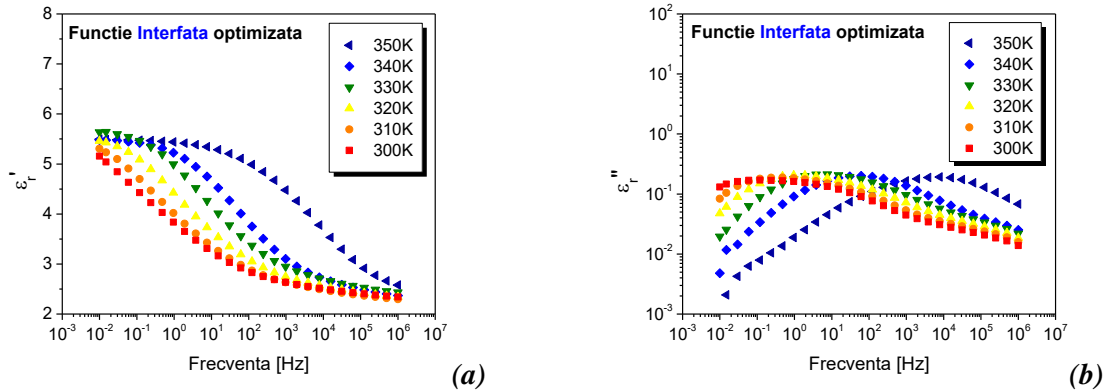
Fig. 5.4. Variation of ε'_r *(a)* and ε''_r *(b)* with frequency for the modeled interface of the PP-SiO$_2$ nanocomposite, using the optimally adjusted LM model [39].

(a) *(b)*
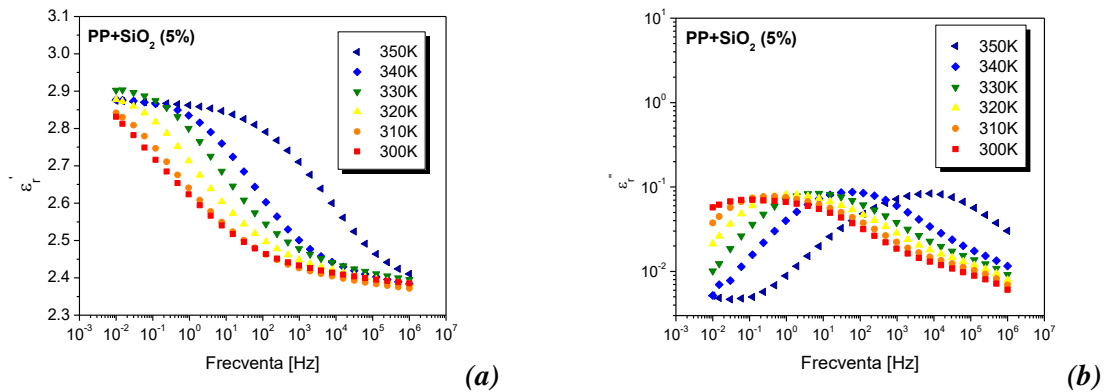
Fig. 5.5. Variation of ε'_r *(a)* and ε''_r *(b)* with frequency for PP-SiO$_2$ nanocomposite [39].

The relaxation frequencies and the displacement of the peaks are the same for both

the interface and the nanocomposite, which indicates that the dielectric response of the interface dominates the dielectric response of the entire nanostructured material. The values of the real and imaginary permittivity of the interface are higher than those of the nanodielectric for any frequency in the range, which shows the influence of the low values of electrical permittivities (real and imaginary part) coming from the polymer matrix on the effectives permittivities of PP-SiO$_2$ nanocomposite [39].

In conclusion, the results of the study presented in this section demonstrate that our approach to finding the optimal scaling factors for adjusting the LM model can be useful to estimate the frequency-dependent permittivity of the interface area found in nanodielectrics by solving an inverse numerical problem.

5.3. VALIDATION OF THE MODEL FOR ESTIMATING INTERFACE ZONE PROPERTIES FOR OTHER NANOCOMPOSITES

To validate the procedure presented in the previous sections, it has also been applied to other nanostructured materials. Another nanostructured material to which the procedure for estimating the properties of the interface area was applied was a nanocomposite having a polymeric matrix of polyethylene (PE) and spherical nanoparticles (15 nm diameter) of TiO$_2$ in a concentration of 2%.

The results obtained for the 2% nanoparticle PE-TiO$_2$ nanodielectric are in accordance with the previously obtained results for the 5% nanoparticle PP-SiO$_2$ nanodielectric and represent a validation of the proposed procedure for estimating the dielectric response area of the spherical particle nanodielectric.

The proposed procedure for estimating the frequency-dependent dielectric behavior of the interface was also tested in the case of another shape of nanoparticles added to the polymer matrix, namely the cylindrical shape (***Fig. 5.6. (a)***) [40]. Although the results are promising, the errors obtained in this case were significantly higher than in the case of spherical particles, reaching up to 46%. A variant considered to improve these results is to modify the computational range by a relatively different orientation of the neighboring nanoparticles (***Fig. 5.6. (b)***), which would contribute to the increase of homogeneity in the elementary cube.
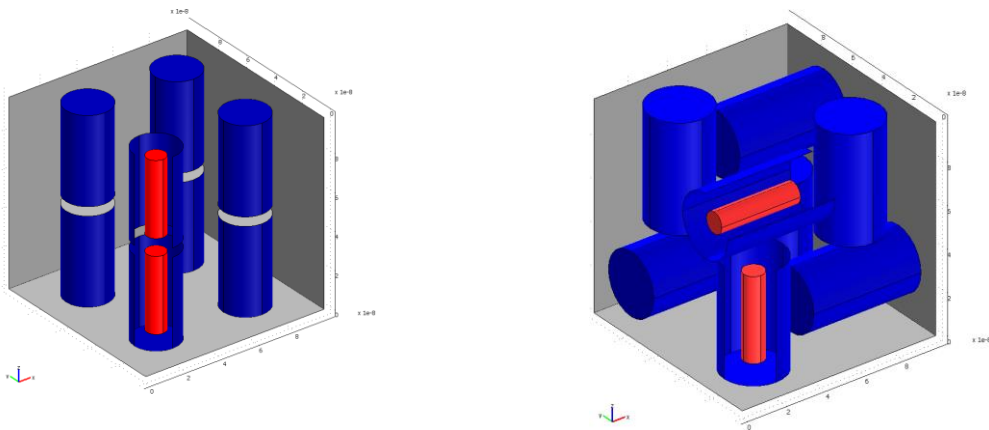
Fig. 5.6. (a) Geometric domain for the numerical model of the PE-TiO$_2$ nanocomposite (cylindrical) [40] (b) the proposed variant for improvement.

CONCLUSIONS

1. GENERAL CONCLUSIONS

1. From the current state of nanostructured materials, in which the emphasis has been on the study of nanostructured dielectric materials, it has been possible to observe the significant number of applications for which they are designed, researched and developed. The applications in the field of electrical engineering where the use of these materials is suitable are numerous and successfully join the field of medical and medical engineering. At the same time, from this bibliographic study it was concluded that the approach of the topic related to the modeling of the phenomena that appear as a result of the interaction of the electromagnetic field with nanostructured dielectric materials is a comprehensive and multidisciplinary topic.

2. The effects of nanostructuring on the polarization and electrical conduction phenomena that occur as a result of the interaction of the electromagnetic field with nanostructured dielectric materials are analyzed in order to understand the electrical and dielectric behavior of these new materials. The study of these effects can be done from two points of view: experimental characterization using dedicated tools and special techniques, or numerical, structural, analytical modeling based on information obtained from experimental determinations. Both research directions were addressed in this paper, as the goal was to understand the behavior of the interface areas that appear in these materials as a result of nanostructuring, the process being a defining one for the final properties and performance of these materials.

3. In the third chapter it was observed how using the experimental analysis method by dielectric spectroscopy provides information about the dynamics of electric charges in the presence of the electric field in nanostructured dielectric materials and implicitly about the effects of nanostructuring on polarization and electrical conduction. This experimental characterization is actual and has been shown to be able to provide a broad perspective on the electrical field behavior of these nanostructured dielectric materials. The completion of the information provided by the analysis method by dielectric spectroscopy with others on the chemical structure and mechanical properties of materials led to the synthesis of conceptual, physical models, and finally numerical models in different regimes of the electromagnetic field.

4. The following conclusions were reached from the analysis of the dielectric spectra obtained on three types of samples of PVC, PE and PP with different nanofillers (SiO_2, TiO_2, Al_2O_3 and cellulosic microfibers):

   - Nanostructuring was observed in all materials analyzed by the presence of a MWS polarization (interfacial) due to the accumulation of electrical charges in the interface areas between nanoparticles and polymers. These electrical charges intensify the other polarization mechanisms that may exist at these frequencies in polymeric nanocomposite materials. At the same time, this relaxation is influenced by the type of nanofiller added in the polymer, this aspect being highlighted especially in nanocomposites based on PE and TiO_2 anatase or rutile type.

   - An α relaxation process could be observed in the low frequency range (specific to crystalline regions) and medium frequency (specific to amorphous regions) for nanocomposites based on semicrystalline polymers such as PP and PE. The presence of maleic anhydride in both pure PE and pure PP has led to an amplification of these α relaxation processes. At high frequencies, radio frequencies, a β relaxation process could be noticed.

   - For pure PVC as well as for PVC-based nanocomposites, a quasi-DC behavior (low frequency dispersion) could be observed.

- The parasitic effect that may occur in some SD measurements as observed in PE-Al$_2$O$_3$ and PP-SiO$_2$ nanocomposites is the electrode polarization, which masks conduction or structural relaxation that may be present at low frequencies. For a better analysis and correlation of the obtained results, the use of the electrical module can eliminate this parasitic effect.
- Temperature and thermal agitation increase can make difficult the orientation of the dipoles and thus decrease the values of the real part of the complex permittivity. Temperature is also an activator of the processes of conduction and dielectric relaxation, which become more significant as thermal agitation intensifies. At the same time, the increase in temperature can activate new inactive dipoles at low temperatures and thus lead to higher values of relative permittivity, as has been observed for example in the case of PP-based nanostructured materials with cellulose microfibers.
- The water present in nanocomposites based on PE, PP and PVC acts as a plasticizer, increasing the free volume and allowing the dipoles to orient themselves more and more easily according to the direction and direction of the electric field. This plasticizing effect of water appears in all the studied materials and is highlighted by the results obtained by SD by dielectric relaxation at low and medium frequencies. On the other hand, if absorbed, bound water is considered as an intruding conductive layer in the insulating polymer, we are talking about a separation zone where electrical charges can accumulate, which intensifies the polarization and conduction phenomena.
- In addition to the qualitative analyzes mentioned above for PVC and PE-based nanocomposites, a quantitative analysis was performed by modeling the dielectric spectra using the HN approximation function and extracting specific energies for electrical conduction or electric polarization processes. This analysis provided a more detailed picture of the charge carriers involved in the molecular dynamics observed by SD, by more accurately identifying the types and parameters of relaxation and conduction present in these nanodielectric materials.

5. The fourth chapter focused on structural characterization and modeling, focusing on the interface area of one of the previously analyzed materials, namely the PP-SiO$_2$ nanocomposite. Thus, a connection was made between the chemical structure of this nanocomposite and its electrical properties, materialized by a structural model of the interface area. This structural model considered the information on the amount of nanoparticles, maleic anhydride, polymer and possible chemical bonds that may form between them, the experimental determinations by TGA that provided information on the water in the nanocomposite and the information taken from the bibliographic study carried out in the second chapter, where models of this interface area were presented. The result obtained initially consisted in identifying the dipoles and modeling their response considering the strength of the chemical and physical bonds at the level of each polar molecule.

6. Furthermore, through the proposed structural model for the PP-SiO$_2$ nanocomposite, it was possible to estimate the value of the electrical permittivity for each of the three layers considered in the nanoparticle-polymer interface. These values of electrical permittivity introduced in a numerically developed model in electrostatic regime led to a difference of less than 3% between the numerically estimated values of electrical permittivity and those determined experimentally at low frequencies (considering the accumulation of space charge in the interface area) and at high frequencies (considering that this electric charge doesn't have enough time to accumulate in the interface area).

7. From the variation of the electric field resulting from the electrostatic numerical model of the PP-SiO$_2$ nanocomposite it was observed that the values of the electric field intensity

are higher in the interface area, in the layers near the nanoparticle, while in the nanoparticle it is very low.

8. In the fifth chapter, a numerical model was developed to highlight the electrical and dielectric properties of the interface area, considering the dispersive nature of the dielectric materials. In this sense, the variation of the electrical permittivity of the interface area with the frequency of the electric field was followed, because, as already highlighted, the dielectric properties of nanocomposite materials are controlled by the polymer-nanoparticle interface. As this was not possible by dielectric spectroscopy or by another experimental analysis technique, the use of numerical modeling was the best solution. In this context, the fifth chapter presents a method for estimating the frequency-dependent dielectric properties of the interface area that exists in PP-SiO$_2$ nanodielectrics. This method consists of an inverse problem of solving a 3D numerical model in quasi-stationary electrical regime, where the subdomains of the nanocomposite (polymer matrix, nanoparticles and interface) are considered dispersive materials.

9. The results obtained with the model developed in quasi-stationary electrical regime showed that the proposed procedure, by solving inverse problems for estimating the frequency-dependent dielectric properties of the polymer-nanoparticle interface, is very useful and reproductible for other types of nanostructured dielectric materials.

2. ORIGINALS CONTRIBUTIONS

- The thesis was based on carrying out an extensive documentary study, consisting of three main parts on the field of nanostructured materials. The first part of the study presents information on the history of nanostructured materials, techniques for obtaining these nanostructures present in nanostructured materials and different classifications of nanostructured materials, depending on the size, content of nanostructures, depending on the type of material used for the matrix. Furthermore, in the second part of the bibliographic study, since the field in which this doctoral thesis is conducted is electrical engineering, the nanostructured materials used in the electrical field are presented, the emphasis being on nanostructured dielectric materials. The last part of the bibliographic study is dedicated to the models developed for nanostructured dielectric materials that are representative of the analysis performed in this paper on the modeling of electromagnetic phenomena in nanodielectrics.

- Carrying out a documentary study on the main phenomena (conduction and electrical polarization) that occur because of the interaction of nanostructured dielectric materials with the electric field, phenomena that can be distinguished in a typical variation with frequency for polymeric dielectrics. Highlighting the main patterns that can be observed after analyzing a dielectric spectrum of a nanostructured dielectric material.

- Carrying out a complex analysis (qualitative - by analyzing the patterns of a dielectric spectrum of a nanostructured dielectric material and quantitative - approximating the dielectric spectra using the HN approximation function and extracting the activation energy of electrical conduction processes or dielectric relaxation) of the results obtained by spectroscopy dielectric for three nanostructured dielectric materials.

- Development of a structural model for a PP-SiO$_2$ nanodielectric where the quantity of nanoparticles, maleic anhydride, polymer and the possible chemical bonds that can be formed between them were considered, as well as the experimental determinations by TGA and the possible polar groups and chemical bonds between them were highlighted. This model was developed using information from structural models for other nanostructured dielectric materials, proposed in the literature.

- Estimation the number of dipoles for the PP-SiO$_2$ nanodielectric, dipoles that can be formed in each of the three layers of the interface area, as well as a calculation to estimate the relative permittivity values of each layer. The calculation of the number of dipoles was made considering that the three layers of the interface have the thicknesses considered in the structural model (1, 5 and 10 nm), and the density of the material in these layers is considered the same as that of the polymer matrix, PP.

- Performing an analytical calculation to estimate the relative electrical permittivity corresponding to each layer of the PP-SiO$_2$ nanodielectric interface, based on the previous dipole number calculation. The values obtained were then used to solve the ENIC model for the PP-SiO$_2$ nanodielectric.

- Propose a procedure for estimating the frequency-dependent dielectric response of the interface area between the nanofiller and the polymer for a PP-SiO$_2$ nanocomposite. The proposed approach involves solving an inverse problem and using a 3D quasi-stationary numerical model, the dielectric spectra obtained for pure PP and the PP-SiO$_2$ nanocomposite and a procedure for adjusting the values obtained for the complex permittivity of the interface area. The procedure is useful because it makes visible the dielectric and dispersive behavior of the interface area, a behavior that cannot be observed by an experimental determination technique.

- Customization of the procedure for estimating the frequency-dependent dielectric response of the interface area between the nanofiller and polymer for a PP-SiO$_2$ nanocomposite for different temperatures, in the range 300 - 350 K.

- Customization of the procedure for estimating the frequency-dependent dielectric response of the interface area between the nanofiller and polymer for other types of nanostructured dielectric materials with different fill (composition or shape) or different polymer matrix.

Some of the studies presented in the thesis, along with others complementary to the topic of this doctoral thesis, have resulted in 22 articles published in the volumes of ISI conferences (11 of them) and in ISI-rated journals (3 of them), the rest of the articles being indexed in international databases (2 of them), but also local (6 of them).

3. FUTURE RESEARCH

- Study the aspects regarding the activation energy of the dielectric relaxation influenced by humidity and / or temperature.
- Development of the structural model of the PP-SiO$_2$ nanodielectric for other nanocomposites, considering the interactions between molecules.
- Development of a numerical model for estimating the dielectric properties for the interface area that simultaneously considers its structure and dynamics, by correlating the numerical model in quasi-stationary regime with the structural model that considers the chemical / physical groups that may occur because of nanostructuring and their dynamics in the presence of an electric field.
- Improving the procedure for estimating the frequency-dependent dielectric response of the interface area of nanodielectrics with cylindrical nanoparticles to better consider the influence of the electric field in materials on the dielectric response of the interface, given the inhomogeneity and anisotropy of the model.
- Creating a fully automated routine to optimize the defined functions by connecting COMSOL Multiphysics and MATLAB software and using optimization algorithms to solve the inverse problem defined in Chapter V to minimize the error between numerical and experimental results.

REFERENCES

[1] J. Jeevanandam, A. Barhoum, Y. S. Chan, A. Dufresne și M. K. Danquah, „Review on nanoparticles and nanostructured materials: history, sources, toxicity and regulations.," *Beilstein journal of nanotechnology,* vol. 9, p. 1050–1074, 2018.

[2] M. Nasrollahzadeh, Z. Issaabadi, M. Sajjadi, S. M. Sajadi și M. Atarod, „Types of Nanostructures," *Interface Science and Technology,* vol. 28, 2019.

[3] A. Biswas, I. S. Bayer, A. S. Biris, T. Wang, E. Dervishi și F. Faupel, „Advances in top–down and bottom–up surface nanofabrication: Techniques, applications & future prospects," *Advances in Colloid and Interface Science,* vol. 170, nr. 1-2, pp. 2-27, 2012.

[4] V. M. Arole și P. S. V. Munde, „Fabrication of nanomaterials by top-down and bottom-up approaches – an overview.," *JAAST:Material Science (Special Issue),* vol. 1, nr. 2, p. 89–93, 2014.

[5] C. Suryanarayana și C. Koch, „Nanocrystalline materials – Current research and future directions," *Hyperfine Interactions ,* vol. 130, nr. 5, 2000.

[6] „An Introduction to Nanoporous Materials," [Interactiv]. Available: https://www.intechopen.com/online-first/an-introduction-to-nanoporous-materials. [Accesat 18 09 2019].

[7] W. J. Orts, J. Shey, S. H. Imam, G. M. Glenn, M. E. Guttman și J.-F. Revol, „Application of Cellulose Microfibrils in Polymer Nanocomposites," *Journal of Polymers and the Environment,* vol. 13, nr. 4, pp. 301-306, 2005.

[8] L. Andrei, F. Ciuprina și D. Panaitescu, „Proprietăți dielectrice ale unor compozite pe bază de polipropilenă," în *Vol. conf. Simpozionul de mașini electrice SME'15*, Bucuresti, 2015.

[9] W. Xu, „Silicon nanowire anode for lithium-ion batteries: fabrication, characterization and solid electrolyte interphase, dissertation," [Interactiv]. Available: https://pdfs.semanticscholar.org/b3f7/60cfc4cd31f8bf63924ebd06c8cbe0263816.pdf. [Accesat 19 09 2019].

[10] J. L. Hass, E. M. Garrison, S. A. Wicher, B. Knapp, N. Bridges și D. N. McIlroy, „Synthetic osteogenic extracellular matrix formed by coated silicon dioxide nanosprings," *Journal of Nanobiotechnology,* vol. 10, nr. 1, p. 6, 2012.

[11] M. S. Akhtar, A. Umar, S. Sood, I. Jung și H. H. Hegazy, „Rapid Growth of TiO2 Nanoflowers via Low-Temperature Solution Process: Photovoltaic and Sensing Applications," *Materials,* vol. 12, nr. 4, pp. 1-14, 2019.

[12] C. P. H. Cury, S. K. Gundappa și W. Fernando, „Nanocomposites : Synthesis , Structure , Properties and New Application Opportunities.," *Materials Research,* vol. 12, nr. 1, pp. 1-39, 2009.

[13] „Global Nanotechnology Market (by Component and Applications), Funding & Investment, Patent Analysis and 27 Companies Profile & Recent Developments - Forecast to 2024," [Interactiv]. Available: https://www.researchandmarkets.com/research/zc7qgf/global?w=5. [Accesat 08 08 2019].

[14] M. Liang și K. Wong, „Improving the long-term performance of composite insulators use nanocomposite: A Review," *Energy Procedia,* vol. 10, pp. 168-173, 2017.

[15] T. Lewis, „Interfaces: nanometric dielectrics," *Journal of Physics D: Applied Physics,* vol. 38, pp. 202 - 212, 2005.

[16] G. Tsagaropoulos și A. Eisenberg, „Dynamic Mechanical Study of the Factors Affecting the Two Glass Transition Behavior of Filled Polymers. Similarities and Differences with Random Ionomers," *Macromolecules,* vol. 28, pp. 6067-6077, 1995.

[17] T. Tanaka, M. Koyako, N. Fuse și Y. Ohki, „Proposal of a multi-core model for polymer nanocomposite dielectrics," *IEEE Trans. Electr. Insul.,* vol. 12, nr. 4, pp. 669-681, 2005.

[18] S. Raetzke și J. Kindersberger, „The Effect of Interphase Structures in Nanodielectrics," *IEEJ Trans.,* vol. 126, p. 1044, 2006.

[19] M. G. Todd și F. G. Shi, „Complex permittivity of composite systems: A comprehensive interphase approach," *IEEE Trans. Dielectr. Electr. Insul.,* vol. 12, nr. 3, p. 601–611, 2005.

[20] F. Ciuprina, L. Andrei, F. Tomescu, I. Plesa și T. Zaharescu, „Electrostatic model of LDPE-SiO2 Nanodielectrics," în *IEEE Intern. Conf. Sol. Dielectr.*, Bologna, Italia, 2013.

[21] I. Plesa, „Influenta umpluturilor anorganice asupra proprietăților dielectrice ale nanocompozitelor polimerice pe baza de polietilena," Teza de doctorat, UPB, Bucuresti, Romania, 2012.

[22] L. Andrei, „Caracterizarea si modelarea nanocompozitelor polimerice folosind analiza prin spectroscopie dielectrica," lucrarea de disertatie UPB, Bucuresti, Romania, 2014.

[23] Y. Huang, T. M. Krentz, J. K. Nelson, L. S. Schadler, Y. Li, H. Zhao, L. C. Brinson, M. Bell și B. B. a. K. Wu, „Prediction of interface dielectric relaxations in bimodal brush functionalized epoxy nanodielectrics by finite element analysis method," în *IEEE Conference on Electrical Insulation and Dielectric Phenomena*, 2014.

[24] „Novocontrol Technologies, WinDETA 5.65 - Owner's manual," nr. 9, 2007.

[25] F. Kremer și A. Schönhals, Broadband Dielectric Spectroscopy, Springer, 2003.

[26] R. M. Hill și L. A. Dissado, „The temperature dependence of relaxation processes," *J. Phys. C Solid State Phys.,* vol. 15, nr. 25, p. 5171–5193, 1982.

[27] „Raport de cercetare, PARTEA a II-a, Diseminarea cunoștințelor și expoaltarea rezultatelor - Metodologii pentru dezvoltarea și caracterizarea de dielectrici din nanocompozite polimerice cu proprietăți electroizolante," CEEX

PoNaDIP 234/2006 Etapa 5, 2008.

[28] WinFIT32, Owner's Manual, Nr. 10, Novocontrol Technologies, 2005.

[29] F. Ciuprina, T. Zaharescu, S. Jipa, I. Plesa, P. Notingher și D. Panaitescu, „Dielectric Properties And Thermal Stability of Gamma-Irradiated Inorganic Nanofiller Modified PVC," *Journal of Radiation Physics and Chemistry,* vol. 79, nr. 3, pp. 379-382, 2010.

[30] F. Ciuprina și L. Andrei, „Effects of Temperature and Nanoparticles on Dielectric Properties of PVC," *UPB Scientific Bulletin Series C: Electrical Engineering,* vol. 77, nr. 4, pp. 383-392, 2015.

[31] L. Andrei și F. Ciuprina, „ANALIZA CONDUCTIVITĂŢII ELECTRICE A NANOCOMPOZITELOR PVC-TiO2 PRIN SPECTROSCOPIE DIELECTRICĂ," în *ACTUALITĂŢI ŞI PERSPECTIVE ÎN DOMENIUL MAŞINILOR ELECTRICE*, Bucuresti, 2020.

[32] L. Andrei și F. Ciuprina, „Temperature influence on electrical conductivity of PVC-TiO2 nanocomposites," în *The 9th International Conference on Modern Power Systems*, Cluj - Napoca, Romania, 2021.

[33] F. Ciuprina și L. Andrei, „Water and Heat Exposure Influence on Dielectric Response of LDPE-Al2O3 Nanocomposites," în *Vol. Conf. IEEE Intern. Sympos. Fundam. Electr. Eng. (ISFEE 2018)*, Bucuresti, Romania, 2018.

[34] F. Ciuprina, L. Andrei, D. Panaitescu și T. Zaharescu, „Temperature Influence on Dielectric Properties of PP-SiO2 Nanocomposites," în *Vol. IEEE Intern. Conf. Diel. (ICD)*, Montpellier, Franta, 2016.

[35] D. Ioan, „Modelarea cuplata electrostatica si mecanica a microcomutatoarelor de RF - Formularea problemei," ToMeMS - Raport intern, Bucuresti, 2012.

[36] A. K. Jonscher, Dielectric Relaxation in Solids, Xi'an Jiaotong University Press, 2007.

[37] L. Andrei și F. Ciuprina, „Dielectric Properties Estimation of Nanodielectric Interphase by Numerical Modeling and Dielectric Spectroscopy," în *Vol. a10a Intern. Symp. Adv. Top. in Electr. Eng. (ATEE 2017)*, Bucuresti, 2017.

[38] „Silica - Silicon Dioxide (SiO2)," [Interactiv]. Available: http://www.azom.com/properties.aspx?ArticleID=1114. [Accesat 15 2 2020].

[39] L. Andrei și F. Ciuprina, „Estimation of Frequency Dependent Dielectric Behavior of PP-SiO2 Nanocomposite Interphase at Different Temperatures," în *Vol. IEEE 2nd Int. Conf. Dielectr. (ICD 2018)*, Budapesta, Ungaria., 2018.

[40] F. Ciuprina și L. Andrei, „Interphase dielectric properties of LDPE-TiO2 nanocomposites," în *Vol. a11a Intern. Symp. Adv. Top. in Electr. Eng. (ATEE 2019)*, Bucuresti, Romania, 2019.